การแยกอิแนนทิโอเมอร์ของแอลกอฮอล์ด้วยแก๊สโครมาโทกราฟีและการศึกษาคิวเอสพีอาร์เพื่อทำนายการแยกอิแนนทิโอเมอร์

นายกฤษติยากรณ์ โตบุญพา

วิทยานิพนธ์นี้เป็นส่วนหนึ่งของการศึกษาตามหลักสูตรปริญญาวิทยาศาสตรมหาบัณฑิต
สาขาวิชาเคมี ภาควิชาเคมี
คณะวิทยาศาสตร์ จุฬาลงกรณ์มหาวิทยาลัย
ปีการศึกษา 2560

ENANTIOMERIC SEPARATION OF ALCOHOLS BY GAS CHROMATOGRAPHY AND QSPR STUDY TO PREDICT ENANTIOMERIC SEPARATION

Mr. Kittiyakorn Toboonpha

A Thesis Submitted in Partial Fulfillment of the Requirements
for the Degree of Master of Science Program in Chemistry
Department of Chemistry
Faculty of Science
Chulalongkorn University
Academic Year 2017

Thesis Title	ENANTIOMERIC SEPARATION OF ALCOHOLS BY GAS CHROMATOGRAPHY AND QSPR STUDY TO PREDICT ENANTIOMERIC SEPARATION
By	Mr. Kittiyakorn Toboonpha
Field of Study	Chemistry
Thesis Advisor	Assistant Professor Aroonsiri Shitangkoon, Ph.D.
Thesis Co-Advisor	Assistant Professor Somsak Pianwanit, Ph.D.

Accepted by the Faculty of Science, Chulalongkorn University in Partial Fulfillment of the Requirements for the Master's Degree

.....Dean of the Faculty of Science
(Professor Polkit Sangvanich, Ph.D.)

THESIS COMMITTEE

.....Chairman
(Assistant Professor Varawut Tangpasuthadol, Ph.D.)

.....Thesis Advisor
(Assistant Professor Aroonsiri Shitangkoon, Ph.D.)

.....Thesis Co-Advisor
(Assistant Professor Somsak Pianwanit, Ph.D.)

.....Examiner
(Assistant Professor Puttaruksa Varanusupakul, Ph.D.)

.....External Examiner
(Assistant Professor Jongkolnee Jongaramruong, Ph.D.)

กฤษติยากรณ์ โตบุญพา : การแยกอิแนนทิโอเมอร์ของแอลกอฮอล์ด้วยแก๊สโครมาโทกราฟีและการศึกษาคิวเอสพีอาร์เพื่อทำนายการแยกอิแนนทิโอเมอร์ (ENANTIOMERIC SEPARATION OF ALCOHOLS BY GAS CHROMATOGRAPHY AND QSPR STUDY TO PREDICT ENANTIOMERIC SEPARATION) อ.ที่ปรึกษาวิทยานิพนธ์หลัก: ผศ. ดร. อรุณศิริ ชิตางกูร, อ.ที่ปรึกษาวิทยานิพนธ์ร่วม: ผศ. ดร. สมศักดิ์ เพียรวณิช, หน้า.

ศึกษาการแยกอิแนนทิโอเมอร์ของแอลกอฮอล์จำนวน 55 ชนิด (แอลิแฟติกแอลกอฮอล์ 13 ชนิด และแอลกอฮอล์ที่มีวงแอโรแมติก 42 ชนิด) ด้วยแก๊สโครมาโทกราฟีโดยใช้ออกตะคิส (2,3-ได-*โอ*-แอซีทิล-6-*โอ-เทอร์ต*-บิวทิลไดเมทิลไซลิล)แกมมาไซโคลเดกซ์ทริน (หรือ GSiAc) เป็นเฟสคงที่ชนิดไครัล ศึกษาแบบโปรแกรมอุณหภูมิ พบว่าสามารถแยกอิแนนทิโอเมอร์ของแอลกอฮอล์ได้ 44 ชนิด มีคู่อิแนนทิโอเมอร์ของแอลิแฟติกแอลกอฮอล์เพียงชนิดเดียวที่สามารถแยกได้อย่างสมบูรณ์คือ 2-เฮกซานอล จากนั้นคัดเลือกแอลกอฮอล์ 25 ชนิดที่มีโครงสร้างคล้ายคลึง 1-ฟีนิลเอทานอลมาศึกษาแบบอุณหภูมิคงที่ สำหรับ 1-ฟีนิลเอทานอลที่มีหมู่แทนที่ชนิดแฮโลเจน พบว่าอุณหภูมิมีผลต่อค่าการแยกอิแนนทิโอเมอร์ในตำแหน่งพารามากที่สุด แต่มีผลต่อค่าการแยกอิแนนทิโอเมอร์ของ 1-ฟีนิลเอทานอลที่มีหมู่แทนที่ชนิดเมทิลหรือไตรฟลูออโรเมทิล ในตำแหน่งออร์โธมากกว่า สำหรับแอลกอฮอล์ที่มีหมู่แทนที่ในตำแหน่งพาราพบว่าสามารถปรับปรุงค่าการแยกอิแนนทิโอเมอร์ได้ดีตามชนิดหมู่แทนที่คือ แฮโลเจน > ไตรฟลูออโรเมทิล > แอลคิล > ฟีนิล สำหรับแอลกอฮอล์ที่มีหมู่แทนที่ชนิดแอลคิลขนาดเล็กที่ตำแหน่งสเทอริโอเจนิก พบว่าสามารถปรับปรุงค่าการแยกอิแนนทิโอเมอร์ได้ดีกว่าหมู่แทนที่ชนิดแอลคิลขนาดใหญ่หรือฟีนิล

ได้พยายามหาแบบจำลองที่สามารถทำนายการแยกอิแนนทิโอเมอร์ของแอลกอฮอล์เหล่านี้โดยใช้เทคนิคการจำลองเชิงโมเลกุลหลายเทคนิค แบบจำลองที่ดีที่สุดที่ได้จากข้อมูลการคำนวณการเข้าจับเชิงโมเลกุล มีความถูกต้องในการทำนาย 83.64 เปอร์เซ็นต์ ได้ทำการจำลองพลวัติเชิงโมเลกุลของแอลกอฮอล์ที่เลือกมาจำนวน 5 ชนิดที่มีค่าการแยกแตกต่างกัน ผลที่ได้ไม่พบความสัมพันธ์กับค่าการแยกอิแนนทิโอเมอร์ สำหรับการศึกษาคิวเอสพีอาร์สามารถหาแบบจำลองที่ดีเยี่ยมในการทำนายอุณหภูมิที่พีกปรากฏสำหรับอิแนนทิโอเมอร์ตัวแรกและอิแนนทิโอเมอร์ตัวหลังได้ โดยมีค่าเฉลี่ยของความคลาดเคลื่อนเพียง 2.30 และ 2.68 องศาเซลเซียส ตามลำดับ

ภาควิชา เคมี	ลายมือชื่อนิสิต .....
สาขาวิชา เคมี	ลายมือชื่อ อ.ที่ปรึกษาหลัก .....
ปีการศึกษา 2560	ลายมือชื่อ อ.ที่ปรึกษาร่วม .....

5772174423 : MAJOR CHEMISTRY
KEYWORDS: ALCOHOL / CHIRAL / CHIRAL ALCOHOLS / CHIRAL SEPARATION / ENANTIOMER / ENANTIOMERIC SEPARATION / CYCLODEXTRIN / GAMMA-CYCLODEXTRIN / QSPR / QSAR / DOCKING / MOLECULAR DOCKING

KITTIYAKORN TOBOONPHA: ENANTIOMERIC SEPARATION OF ALCOHOLS BY GAS CHROMATOGRAPHY AND QSPR STUDY TO PREDICT ENANTIOMERIC SEPARATION. ADVISOR: ASST. PROF. AROONSIRI SHITANGKOON, Ph.D., CO-ADVISOR: ASST. PROF. SOMSAK PIANWANIT, Ph.D., pp.

Enantiomeric separation of 55 alcohols (13 aliphatic alcohols and 42 alcohols of aromatic structure) was studied by gas chromatography using octakis(2,3-di-*O*-acetyl-6-*O*-*tert*-butyldimethylsilyl)-γ-CD (or GSiAc) as a chiral stationary phase. For separation under temperature program, 44 alcohols could be enantioseparated. The only aliphatic alcohol that could be completely separated into their enantiomers was 2-hexanol. Twenty-five alcohols, based on 1-phenylethanol, were selected to study under isothermal conditions. For halogen-substituted 1-phenylethanols, temperature strongly affected enantioselectivities of *para*-substituted alcohols. However, temperature affected enantioselectivities of methyl- or trifluoromethyl-substituted alcohols at *ortho*-position more than other positions. For *para*-substituted alcohols, enantioseparations could be improved with the substituent in the order of halogen > trifluoromethyl > alkyl > phenyl. In addition, temperature affected enantioselectivities of alcohols with small alkyl substitution at the stereogenic center rather than bulky alkyl or phenyl group.

Attempt to find model that can predict enantioseparations of these alcohols was made using several molecular modeling techniques. From molecular docking calculations, the best predictive model has an accuracy of 83.64 %. MD simulations were applied for only 5 selected alcohols with different enantioselectivities and the results showed no relationship with enantioselectivity. For QSPR studies, excellent models to predict elution temperatures of the less retained and the more retained enantiomers were developed with the average errors of only 2.30 and 2.68 degrees Celsius, respectively.

Department:	Chemistry	Student's Signature	.....
Field of Study:	Chemistry	Advisor's Signature	.....
Academic Year:	2017	Co-Advisor's Signature	.....

ACKNOWLEDGEMENTS

First of all, I am grateful to my thesis advisor, Assistant Professor Dr. Aroonsiri Shitangkoon, for valuable suggestion and knowledge. During the three years of my study, she gives comments, supervision all step of this research, and careful proofreading of this thesis.

I would like to thank my co-advisor, Assistant Professor Dr. Somsak Pianwanit, who provides physical chemistry knowledge, guidance and suggestions during QSPR and molecular modeling work as well as careful proofreading of this thesis.

I would also like to thank my thesis committee, Assistant Professor Dr. Varawut Tangpasuthadol, Assistant Professor Dr. Puttaruksa Varanusupakul and Assistant Professor Dr. Jongkolnee Jongaramruong for their useful suggestions and comments.

My special thanks to Professor Gyula Vigh (Texas A&M University, USA) for offering the cyclodextrin derivative used in this research and thankful to Department of Chemistry, Chulalongkorn University for providing equipment and financial support. Thanks to the staffs for continuous support.

Finally, many thanks to all members of chiral separation group, family and all my friends for great advice, encouragement, love and support.

CONTENTS

Page

LIST OF TABLES

LIST OF FIGURES

CHAPTER I

Introduction

Alcohols are important compounds and play significant roles in many fields such as pharmaceuticals, agrochemicals and biochemistry. In biochemistry, chiral compound can mediate different or opposite effects such as *S*-configuration of penicillamine is effective for the treatment Rheumatoid arthritis, but *R*-configuration is highly toxic [1]. For chiral alcohols may have different effects in living systems. Each enantiomer of chiral alcohol can show different bioactivity, toxicity or clinical activity. For example, (*S*)-timolol is effective for the treatment of cardiovascular disease, while (*R*)-timolol is effective for the treatment of glaucoma [2]. Another example is propranolol which is used to treat high blood pressure and anxiety symptoms. It was found that (*S*)-(–)-propranolol is more potent than (*R*)-(+)-propranolol, in addition, the elimination of (*S*)-(–)-propranolol from the body is more difficult than the (*R*)-(+)-enantiomer. However, both enantiomers showed the same local anesthetic effect [3]. Therefore; it is necessary to use these drugs in the form of pure single enantiomer to avoid the side effects and undesired toxicity. Consequently, the synthesis of pure single enantiomer and the determination of enantiomeric purity are important as well.

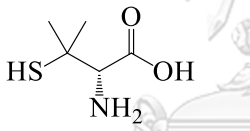

(*S*)- penicillamine

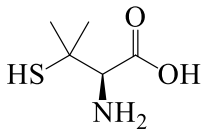

(*R*)- penicillamine

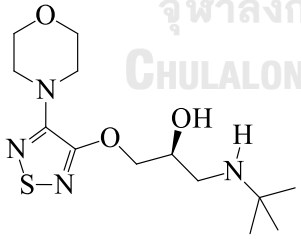

(*S*)-timolol

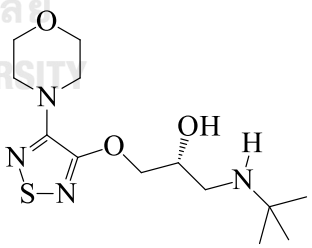

(*R*)-timolol

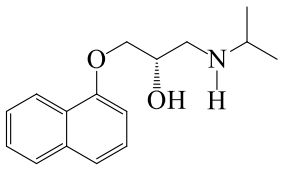

(*S*)-(–)-propranolol

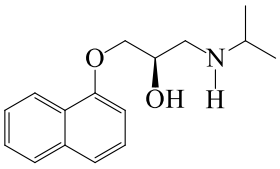

(*R*)-(+)-propranolol

Figure 1.1 Structures of penicillamine, timolol and propranolol

Analysis of enantiomer purity using separation techniques, such as chromatography or electrophoresis, could be performed directly or indirectly. The direct method using chiral selectors as stationary phases or chiral resolving agents was achieved with high performance liquid chromatography (HPLC) [4-6], capillary electrophoresis (CE) [7-10] or gas chromatography (GC) [11-16]. For volatile and thermally stable organic compounds, such as alcohols, GC is the preferred technique with the use of derivatized cyclodextrins (CDs) as chiral stationary phases [8-17].

There were several studies regarding the prediction of chromatographic retention time of various substances such as phenols [18], derivatized steroids [19], pesticides [20], etc. The prediction of enantioselectivities was also attempted using many techniques [21, 22]. Quantitative structure-property relationship (QSPR) [23] is a popular and widely used technique for predicting chemical properties of compounds. QSPR is created by calculating the structural properties of the substances and then using a statistical method to find the relationship between the calculated structural properties and the interested properties. The relationship is described in the form of an equation or mathematical model that can be used to predict the interested properties. If an enantiomeric separation in various environments could be predicted accurately, it will be very useful (save time and save cost) for selecting suitable techniques or methods for the analysis of enantiomers.

Previously, the enantiomeric separations of alcohols were mostly reported using β-CD derivatives as chiral stationary phases [16]. However, γ-CD derivatives showed good enantioselectivities towards several types of analytes [17]. In addition, the study of enantioselective reaction of lipase B from yeast species *Candida antarctica* (CALB) using three-dimensional quantitative structure-activity relationship (3D-QSAR) technique showed good prediction of enantiomeric ratio [22]. Moreover, the study on predictive retention time of steroids from GC analysis using multiple linear regression (MLR), partial least squares regression (PLS) and artificial neural networks (ANNs) methods showed that ANNs models perform better than MLR and PLS [19]. However, there is no report on the relationship between the properties of alcohols and experimental enantioselectivities. The effect of relationship between enantioselectivity and difference binding energy of the enantiomer pair with the CD derivative on GC separation has not been reported as well.

In this work, the aim was to study the enantiomeric separation of 25 alcohols by GC using octakis(2,3-di-*O*-acetyl-6-*O*-*tert*-butyldimethylsilyl)-γ-CD mixed in polysiloxane as a chiral stationary phase. All alcohols are 1-phenylethanol derivatives with different type and position of substituents. The effects of alcohol structure as well as column temperature towards retention factor and enantioselectivity were studied. Moreover, QSPR technique was also applied to find the relationship between the properties of enantiomer of alcohols and enantioselectivity, which would be very useful for predicting the enantioseparation of alcohols. The data can be used to select

appropriate stationary phase for separate alcohols and other functional groups in the future.

CHAPTER II
Theory

2.1 Enantiomeric separation by gas chromatography

Generally, there are two approaches for an analytical separation of enantiomers, direct and indirect approaches. In the direct approach, enantiomers are separated directly by using chiral stationary phase or chiral selector. On the other hand, the indirect approach uses the chiral reagent to react with enantiomers to transform them into diastereomers, which have different chemical and physical properties and can be separated by conventional techniques. Limitations of indirect method are demand of the pure chiral reagent, the availability of functional groups of enantiomers for the reaction and long analysis time for preparation and identification. Therefore, direct separation using high performance liquid chromatography (HPLC) [4-6], capillary electrophoresis (CE) [7-10] or gas chromatography (GC) [11-16] are preferred techniques for the analysis of enantiomeric purity of chiral analytes. For volatile and thermally stable organic compounds, GC is the most suitable technique.

Among several types of chiral stationary phases, cyclodextrin (CD) derivatives are among the most commonly used chiral stationary phases in GC because of their ability to form inclusion complexes with various types of substances. CDs can be modified into several derivatized forms, thus offering various types of selectivities. In addition, CD derivatives can be operated at wide operating temperature range [24, 25].

2.2 Cyclodextrin

Cyclodextrins (CDs) [26] are cyclic oligosaccharides made from enzyme digestion of linear amylose component of starch. The CD subunits are D-glucoses connected by α-(1,4)-glycosidic bonds to form a cyclic molecule. CDs are truncated cone shaped with central cavity with the hydrophobic property inside the cavity and the exterior surface shows hydrophilic property (Figure 2.1). This characteristic provides the inclusion of nonpolar compound (guest) inside the cavity of CD (host). The primary hydroxyl groups at C6 position of CD molecule are at the narrow edge but the secondary hydroxyl groups at C2 and C3 positions are at the wider edge.

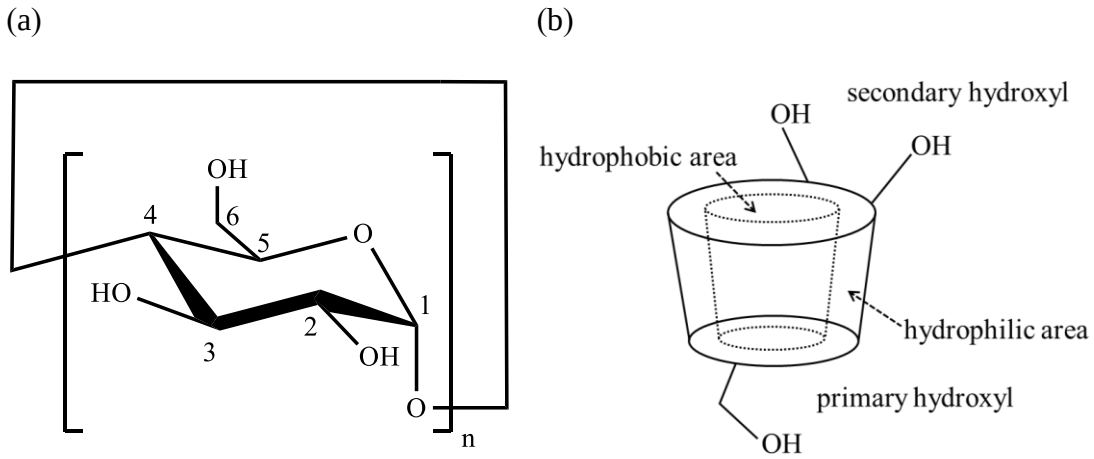

Figure 2.1 (a) A structure of CD molecule with n glucose units (b) truncated cone shaped of CD.

The size of CD depends on the number of glucose units in its molecule. Three most common CDs compose of six, seven and eight D-glucose units and are called α-, β- and γ-CDs, respectively. Some important properties of these CDs are shown in Table 2.1.

Table 2.1 Some important properties of α-, β- and γ-CDs [27, 28]

properties	cyclodextrin (CD)		
	α	β	γ
number of glucose units	6	7	8
molecular weight	972.86	1135.01	1291.15
internal diameter (Å)	4.7 – 5.3	6.0 – 6.5	7.5 – 8.3
cavity depth (Å)	7.9	7.9	7.9
volume of cavity	174	262	427
water solubility at room temp (g/100 mL)	14.50	1.85	23.20
decomposition (°C)	278	299	267

CDs can be modified to improve their properties, such as solubility, decomposition temperature or selectivity by substituting various functional groups on the hydroxyl group. Generally, the primary hydroxyl group at C6 positions of each glucose unit are modified with bulky size or long chain alkyl groups to change the shape or conformation of the CDs, while the secondary hydroxyl at C2 and C3 positions of

each glucose unit are modified with small alkyl or acyl groups to improve the enantioselectivities.

2.3 GC separation of enantiomers using CD derivatives

Most native CDs are not suitable to use as stationary phases in GC capillary column because they are solid at room temperature and have limited operating temperature. However, native CDs can be modified by chemical reaction such as alkylation, acylation, or silylation to obtain CD derivatives [27, 29, 30]. The reaction mostly occurs at the hydroxyl groups on C2, C3 and/or C6 positions of CD. CD derivatives have different functional groups, shape and size from the native CDs and they show different enantioselectivities due to the interactions between CD derivatives and analytes are changed. Several derivatized CDs are solid at room temperature, these CDs cannot be coated directly onto the wall of a GC capillary column. Thus, they are often mixed with achiral polysiloxane in order to improve their coating properties before being used as stationary phase over wider operating temperature range [31-33]. The nonpolar substituents replaced at the hydroxyl groups of CD could improve the solubility of CD in nonpolar polysiloxanes as well.

Previous research concerning the enantiomer separation by GC using various derivatized CDs of different size, type and position of substituent as stationary phases will be mentioned.

In 1996, Bicchi and co-workers [11] studied the enantioseparation of lactones, esters, ketones and alcohols by GC using *O-tert*-butyldimethylsilyl-CD derivatives as stationary phases. Four CD derivatives of different size (β, γ) and different substituent (methyl, ethyl) at C2 and C3 of glucose units are: METBS-β-CD, METBS-γ-CD, ETTBS-β-CD and ETTBS-γ-CD. Each CD was mixed with polysiloxane of different polarity (PS-347.5, PS-086 and OV-1701) before using as stationary phases. It was found that enantiomers of chiral analytes could be separated with β-CD derivatives better than with γ-CD derivatives. The effect of CD substituent was shown. ETTBS-β-CD with ethyl groups could be operated at lower column temperature while providing similar or better enantioselectivity than the METBS-β-CD with smaller methyl substituents. The polarity of polysiloxane also affected the enantioseparation. It was found that enantioselectivities obtained from high polarity OV-1701(polycyanopropylphenyl(vinyl)methylsiloxanes) was lower than those obtained from low polarity PS-347.5 (polymethylsiloxanes) and PS-086 (polymethylphenylsiloxanes).

In 2005, Takahisa and Engel [12] synthesized 2,3-di-*O*-methoxymethyl-6-*O*-*tert*-butyldimethylsilyl-γ-CD and used as a GC stationary phase for enantiomer separation of 125 analytes including alcohols, aldehydes, ketones, organic acids, esters

and lactones. It was found that enantiomers of all types of analytes could be separated with this new CD derivative. It provided very high enantioselectivities towards some hydroxyketones and branched chain methylketones and showed good enantioselectivities towards alcohols and halogenated analytes.

In 2010, Huang, Zhang and Armstrong [34] produce a new type of gas chromatographic chiral stationary phase. Ionic cyclodextrins which are permethylated mono-6-(butylimidazolium)-cyclodextrin (BIM-BPM) and permethylated mono-6-(tripropylphosphonium)-cyclodextrin (TPP-BPM) were synthesized and dissolved in various dicationic and tricationic ionic liquids (ILs) and examined as GC chiral stationary phases. The performance of these columns was compared to that of their neutral cyclodextrin containing IL-based predecessors. The new ionic liquid-based stationary phase exhibits broader enantioselectivities, up to seven times higher efficiencies, and greater thermal stabilities. When compared to the commercial polysiloxane-based CSPs with analogous chiral selectors. it shows different enantioselectivities and more symmetric peak shapes. The separation enhancements are usually found for more polar analytes.

In 2014, Jongjitwattana [16] studied the enantioseparation of underivatized 1-phenylethanols with different types and position of substituents and their corresponding trifluoroacetyl (TFA) and trimethylsilyl (TMS) derivatives by GC using 2,3-di-*O*-acetyl-6-*O*-*tert*-butyldimethylsilyl-β-CD as a stationary phase. It was found that the number of underivatized alcohols could be enantioseparated than the number of TFA or TMS derivatives. The effect of temperature on enantioselectivity was noticeable with the *meta*-substituted underivatized alcohols and the *para*-substituted derivatized alcohols. The advantages of alcohol derivatization were the more symmetrical peak shapes and, in some cases, the improved enantioselectivity. Enantiomers of many TFA-derivatized alcohols could be completely separated in shorter analysis time than underivatized alcohols.

2.4 Thermodynamic investigation for enantioseparation by GC

The mechanisms of chiral separation by CD derivatives on GC are not well understood. However, some explanations could be obtained based on thermodynamic studies. In general, it is realized that the direct enantiomeric separation occurs via the formation of temporary reversible diastereomeric complexes between a chiral selector and an enantiomer. For the complex formation, temperature is an important factor influencing retention factor, enantioselectivity and resolution of analytes. The chemical equilibrium associated between a chiral selector and an enantiomer can be described by van’t Hoff approach as follow [31, 35].

$$-\Delta(\Delta G) = RT \cdot \ln\alpha = RT \cdot \ln\left(\frac{k'_2}{k'_1}\right) \qquad (1)$$

Where α is the separation factor or selectivity calculated from the ratio of k′ of two enantiomers

k' is the retention factor or capacity factor of each enantiomer calculated from solute retention time according to

$$k' = \frac{t_R - t_M}{t_M}$$

t_R is the retention time of an enantiomer or an analyte

t_M is the time for mobile phase or an unretained compound to travel at the same distance as an analyte

R is the universal gas constant (1.987 cal/mol·K)

T is the absolute temperature (K)

1,2 arbitrarily to the less and the more retained enantiomers, respectively

Combining equation (1) with the Gibbs-Helmholtz equation (2), given equation (3):

$$-\Delta(\Delta G) = -\Delta(\Delta H) + T \cdot \Delta(\Delta S) \qquad (2)$$

$$RT \cdot \ln\alpha = -\Delta(\Delta H) + T \cdot \Delta(\Delta S) \qquad (3)$$

Rewrite equation (3) as show below:

$$\ln\alpha = \frac{-\Delta(\Delta H)}{RT} + \frac{\Delta(\Delta S)}{R} \qquad (4)$$

Where $\Delta(\Delta H)$ is the difference in enthalpy values for an enantiomeric pair

$\Delta(\Delta S)$ is the difference in entropy values for an enantiomeric pair

From equation (4), $\Delta(\Delta H)$ and $\Delta(\Delta S)$ could be calculated from the slope and y-intercept of the ln α vs 1/T plot. Thermodynamic parameters from these plots are not always possible due to the nonlinearity of the plots when using chiral selector in a diluted stationary phase. So, this method is valid when using undiluted chiral selector.

Nevertheless, thermodynamic parameters could be calculated from the slope and y-intercept of the ln k′ vs 1/T plot from equation (7), which could be derived from the combination of equations (5) and (6) as shown below:

$$-\Delta G = RT \cdot \ln K = RT \cdot \ln (k' \cdot \beta) \quad (5)$$

$$\Delta G = \Delta H - T \cdot \Delta S \quad (6)$$

$$\ln k' = \frac{-\Delta H}{RT} + \frac{\Delta S}{R} - \ln \beta \quad (7)$$

Where K is the distribution coefficient of a chiral analyte between the gas and the liquid phases

β is a constant called phase ratio (the ratio of mobile phase volume to stationary phase volume)

ΔH is enthalpy change resulting from the interaction of the enantiomer with the stationary phase. ΔH value describes the degree of the interaction strength. The large negative ΔH value indicates high strength of interaction between analyte and stationary phase.

ΔS is enthalpy change resulting from the interaction of the enantiomer with the stationary phase. ΔH value describes the degree of which the solute structure influences the interaction.

2.5 Molecular modeling studies for enantioseparation

The success in separation of enantiomers using CD derivatives as chiral stationary phase is certainly related to different interaction between CD molecule and each couple of enantiomers. However, such interactions are not yet clearly understood due to limitation in experimental techniques and equipment. Therefore, molecular

modeling methods, e.g. molecular docking and molecular dynamics simulation, have been used to shed light on this topic. In addition, quantitative structure-property relationship (QSPR) or quantitative structure-retention relationship (QSRR) methods have also been used to predict the retention time for each enantiomer as well as to understand structural features of the chiral recognition mechanism.

In QSPR study, various chemical and physical properties of a series of analytes are calculated and then statistical method is applied to find relationship between the calculated structural properties and the interested properties, e.g. retention time, elution temperature. The relationship is expressed in a form of an equation or mathematical model that can be used to quantitatively predict the property. Interesting QSPR/QSRR research works related to enantioseparation are summarized as follow.

In 2009, Braiuca and co-workers [22] built a three-dimensional quantitative structure-activity relationship (3D-QSAR) model to predict the enantioselectivity of *Candida antarctica* Lipase B (CALB) toward 19 amines and alcohols in the enzymatic acylation reactions. This CALB enzyme catalyzes reaction of *R* and *S* enantiomers of each substrate at different reaction rate. Differential molecular interaction fields, which are different in interaction fields between *R* and *S* enantiomer of each substrate, were used to correlate with enantiomeric ratio. The obtained model has good predictive ability with q^2 (cross-validated r^2) value of 0.78

In 2012, Fragkaki and co-workers [19] built a model to predict retention time (GC technique) of trimethylsilylated anabolic androgenic steroids using several structural properties affecting retention time such as Henry's law constant, boiling point, dipole-dipole energy etc. and using several statistical methods such as multiple linear regression (MLR), partial least squares (PLS) and artificial neural networks (ANNs) to find the relationship. Based on the statistical results, ANNs models performed better than MLS and PLS and the variables most affected to retention time prediction is the moment of inertia along the Y axis (PMI Y) and minimum electrotopological index (gmin).

In 2013, Zahra Dashtbozorgi and co-workers [20] performed QSRR study to predict retention time (t_R) of 368 pesticide residues in animal tissues separated by gas chromatography-mass spectrometry (GC–MS). The genetic algorithm-partial least squares (GA-PLS) method was used for variable selection. Then PLS, artificial neural network (ANN) and support vector machine (SVM) methods were applied to build a model. The correlation coefficients (R) between experimental and predicted t_R for the prediction set by PLS, ANN and SVM are 0.907, 0.963 and 0.985 respectively. Results obtained reveal the superiority of the SVM model over PLS and ANN.

2.5.1 Molecular docking

Molecular docking is a technique to predict the binding between two molecules. The docking calculation consists of two main processes, configuration sampling and score evaluation. Since there are enormous possible configurations for the binding, it is impossible to explore all these configurations. Therefore, an efficient sampling technique must be used to limit computational time and resources. In the AutoDock 4.2, genetic algorithm is used for configuration sampling. For the score evaluation, it is used to determine how good is the binding of each configuration so that the best binding configuration can be chosen. In the AutoDock 4.2, score is evaluated from binding interaction energy, which mainly composes of steric and electrostatic interaction energy [36, 37]. For steric energy, the Lennard-Jones 12-6 pair potentials are used to model the van der Waals forces and the 12-10 form is used to model hydrogen bonds. For electrostatic energy, the Coulomb potential is used.

In AutoDock 4.2 software, numerous interaction energies for each configuration must be calculated. Therefore, grid base energy evaluation is used to reduce computational time. Steric and electrostatic energy around the receptor (host molecule) are pre-calculated and stored as map files. A grid map consists of a three dimensions lattice of the regularly space points, surrounding and centered on some or all region of the host molecule. The default grid point spacing is 0.375 Å. At each lattice point, both steric and electrostatic interaction energies between the probe atom and CD atoms is calculated using the Lennard-Jones 12-6 potential and is assigned to that lattice point.

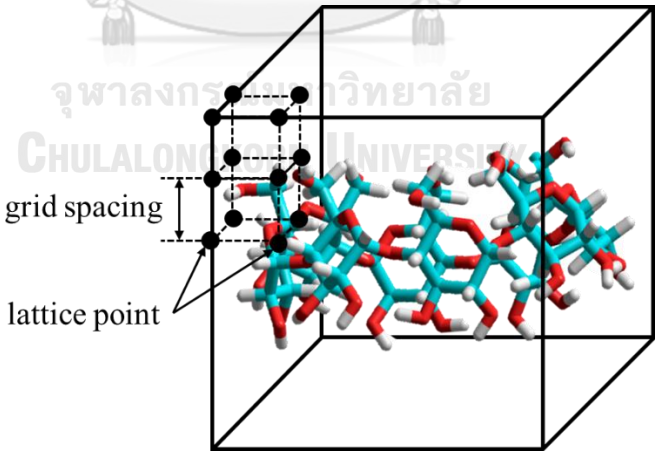

Figure 2.2 Grid base energy evaluation in AutoDock

2.5.2 Molecular dynamics simulation

Molecular dynamics (MD) simulation [38] is a useful computational technique to simulate physical movements of atoms and molecules with respect to time according to Newton's equations of motion [39]. A trajectory is generated consisting of positions and velocities along simulation time. Analysis of the trajectory enables the study of interaction and dynamics of guest molecule inside host molecule at molecular level.

2.5.3 Statistical methods for QSPR

Binding energy calculated from molecular docking or MD simulation and structural properties are used to find relationship with enantioselectivity or elution temperature from experiment. Multiple linear regression (MLR) analysis and genetic function approximation (GFA) method were employed to give the QSPR model.

GFA algorithm is a technique for generating statistical models of data using the process of evolution [40-42] derived from earlier work on evolutionary spline modeling [43, 44]. This method stands in contrast to techniques such as partial-least squares regression [45, 46] or neural-network modeling [47], which deterministically construct a single functional model of a data set from a given set of first principles and assumptions. GFA uses a nondeterministic process like to evolution to guide the development of a population of many statistical models. Further, the method is naturally conformable to the construction of nonlinear models of data. The population will develop novel, easily interpreted, and statistically-reasonable nonlinear models.

CHAPTER III

Experiment

3.1 Chiral alcohols

Chiral alcohols used in this work were previously prepared by Iamsam-ang [48], Konghuirob [49] and Jongjitwatana [16]. Chiral alcohols were synthesized from their corresponding ketones by sodium borohydride reduction [16]. The identification of alcohol products was done by ^{1}H- and ^{13}C-NMR (Bruker AV-400 spectrometer) using deuterated chloroform ($CDCl_3$) as a solvent. The alcohol analytes were diluted in dichloromethane to obtain the final concentration of ~0.1 mg/mL and were analyzed by GC without derivatization. The structures of all alcohols used in this work are shown in Table 3.1.

Table 3.1 Structure, abbreviation and name of chiral alcohols

no.	structure	abbreviation	name
1	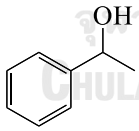	**1**	1-phenylethanol (reference compound)
1-phenylethanols with substitution on the aromatic ring			
2	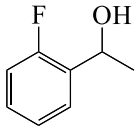	**2F**	1-(2-fluorophenyl)ethanol
3	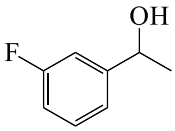	**3F**	1-(3-fluorophenyl)ethanol
4	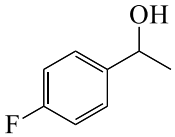	**4F**	1-(4-fluorophenyl)ethanol

no.	structure	abbreviation	name
5	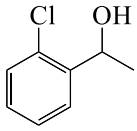	**2Cl**	1-(2-chlorophenyl)ethanol
6	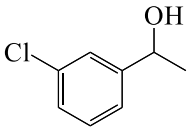	**3Cl**	1-(3-chlorophenyl)ethanol
7	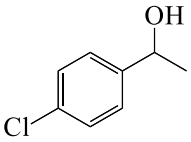	**4Cl**	1-(4-chlorophenyl)ethanol
8	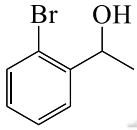	**2Br**	1-(2-bromophenyl)ethanol
9	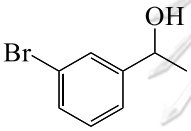	**3Br**	1-(3-bromophenyl)ethanol
10	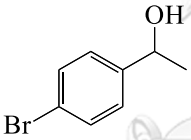	**4Br**	1-(4-bromophenyl)ethanol
11	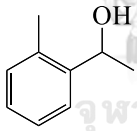	**2Me**	1-(2-methylphenyl)ethanol
12	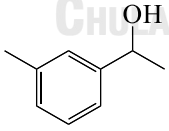	**3Me**	1-(3-methylphenyl)ethanol
13	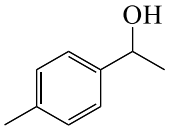	**4Me**	1-(4-methylphenyl)ethanol
14	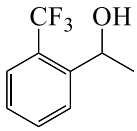	**2CF3**	1-(2-trifluoromethylphenyl) ethanol
15	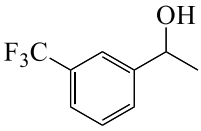	**3CF3**	1-(3-trifluoromethylphenyl) ethanol

no.	structure	abbreviation	name
16	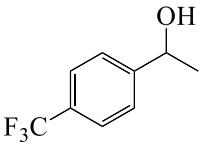	**4CF3**	1-(4-trifluoromethylphenyl) ethanol
17	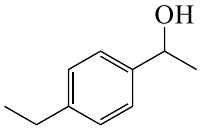	**4Et**	1-(4-ethylphenyl)ethanol
18	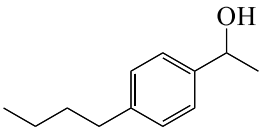	**4Bu**	1-(4-butylphenyl)ethanol
19	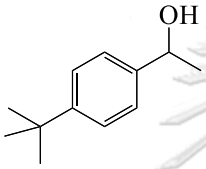	**4tBu**	1-(4-*tert*-butylphenyl)ethanol
20	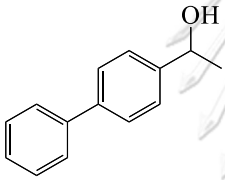	**4Phe**	1-(4-diphenyl)ethanol
21	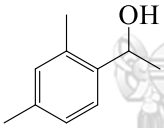	**24Me**	1-(2,4-dimethylphenyl)ethanol
22	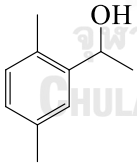	**25Me**	1-(2,5-dimethylphenyl)ethanol
23	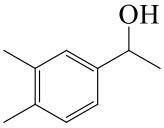	**34Me**	1-(3,4-dimethylphenyl)ethanol
other alcohols			
24	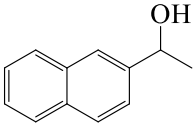	**2**	1-(2-naphthyl)ethanol

no.	structure	abbreviation	name
25	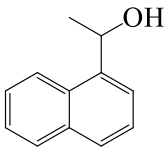	**3**	1-(1-naphthyl)ethanol
26	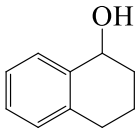	**4**	1,2,3,4-tetrahydro-1-naphthol
27	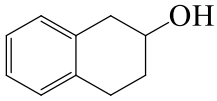	**5**	1,2,3,4-tetrahydro-2-naphthol
28	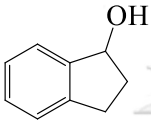	**6**	1-indanol
29	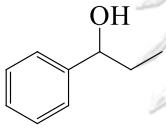	**7**	1-phenyl-1-propanol
30	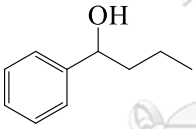	**8**	1-phenyl-1-butanol
31	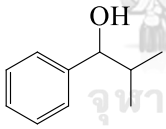	**9**	2-methyl-1-phenyl-1-propanol
32	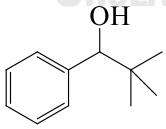	**10**	2,2-dimethyl-1-phenyl-1-propanol
33	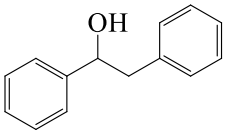	**11**	1,2-diphenylethanol
34	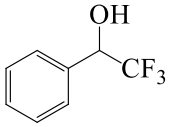	**12**	2,2,2-trifluoro-1-phenylethanol

no.	structure	abbreviation	name
35	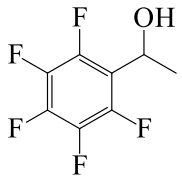	**13**	1-(pentafluorophenyl)ethanol
diphenylmethanols with mono-substitution on one aromatic ring			
36	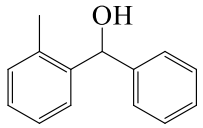	**2MeBen**	phenyl-*o*-tolyl-methanol
37	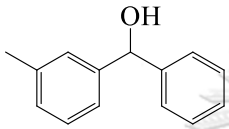	**3MeBen**	phenyl-*m*-tolyl-methanol
38	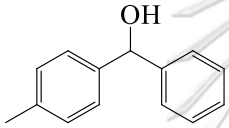	**4MeBen**	phenyl-*p*-tolyl-methanol
39	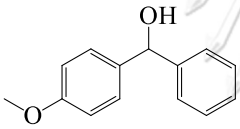	**4OMeBen**	(4-methoxyphenyl)phenyl-methanol
40	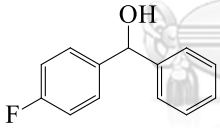	**4FBen**	(4-fluorophenyl)phenyl-methanol
41	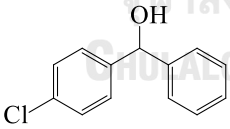	**4ClBen**	(4-chlorophenyl)phenyl-methanol
42	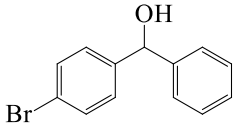	**4BrBen**	(4-bromophenyl)phenyl-methanol
n-alkyl alcohols			
43	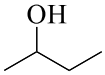	**2but**	2-butanol
44	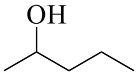	**2pen**	2-pentanol

no.	structure	abbreviation	name
45	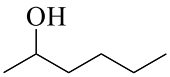	**2hex**	2-hexanol
46	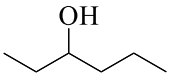	**3hex**	3-hexanol
47	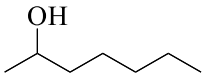	**2hep**	2-heptanol
48	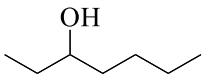	**3hep**	3-heptanol
49	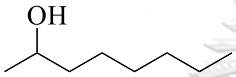	**2oc**	2-octanol
50	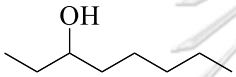	**3oc**	3-octanol
51	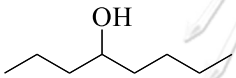	**4oc**	4-octanol
52	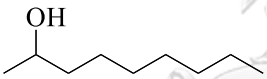	**2non**	2-nonanol
53	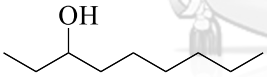	**3non**	3-nonanol
54	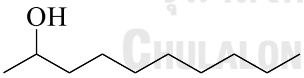	**2dec**	2-decanol
55	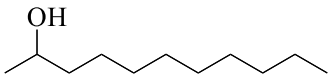	**2undec**	2-undecanol

3.2 Gas chromatographic analysis

3.2.1 Coating a capillary column

A deactivated fused silica capillary column of 15 m long and 0.25 mm I.D. (Agilent) was coated with a 0.25 μm film thickness of stationary phase using a static method. Octakis(2,3-di-*O*-acetyl-6-*O*-*tert*-butyldimethyl)-γ-CD (GSiAc) was received from Professor Gyula Vigh (Texas A & M University, USA) and used as a chiral selector in the stationary phase. The stationary phase was a mixture of 36.5% GSiAc in polysiloxane OV-1701 (7% phenyl, 7% cyanopropyl, 86% dimethylpolysiloxane, Supelco). The coated column was conditioned at 220 °C until the baseline was stable. The column efficiency was evaluated at various temperatures using *n*-alkanes before usage.

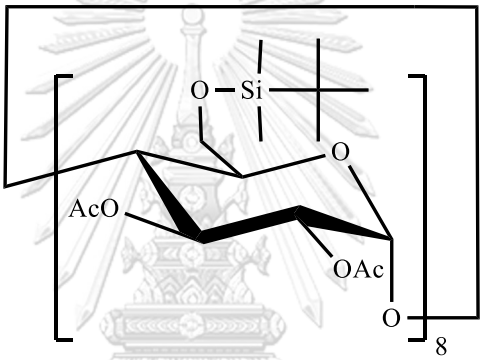

GSiAc

3.2.2 Instrumentation and GC conditions

All analytes were performed on an Agilent 6890 series gas chromatograph equipped with a split injector and a flame ionization detector. Both injector and detector temperatures were set at 250 °C. A split ratio was adjusted to 100. The hydrogen carrier gas was used at an average linear velocity of 50 cm/sec. All 55 chiral alcohols were analyzed in duplicate using a temperature program from 40 °C to 220 °C at a rate of 3.3 °C/min. The elution temperatures for all eluted peaks were calculated and were used further in QSPR model. Twenty-five selected alcohols (**1**, **7**, **8**, **9**, **10**, **22**, **2F**, **3F**, **4F**, **2Cl**, **3Cl**, **4Cl**, **2Br**, **3Br**, **4Br**, **2Me**, **3Me**, **4Me**, **2CF3**, **3CF3**, **4CF3**, **4Et**, **4Bu**, **4tBu** and **4Phe**) were analyzed, at least in duplicate, isothermally every 10 °C interval at 6-8 different temperatures. Retention factors (k'), selectivity (α) and resolution (Rs) were calculated from the chromatogram from each run.

3.3 Molecular modeling

3.3.1 GSiAc structure

The three-dimensional structure of GSiAc was constructed using the X-ray crystallographic data of non-modified γ-CD (Figure 3.1) as a template. All hydroxyl hydrogen atoms in the template structure at the 2 and 3 positions were replaced with acetyl groups and those at the 6 positions were replaced with *tert*-butyldimethylsilyl groups. Then, the structure was geometrically optimized with semi-empirical AM1 method using HyperChem software (Figure 3.2), and with semi-empirical PM7 method using MOPAC2016 (Figure 3.3) [50].

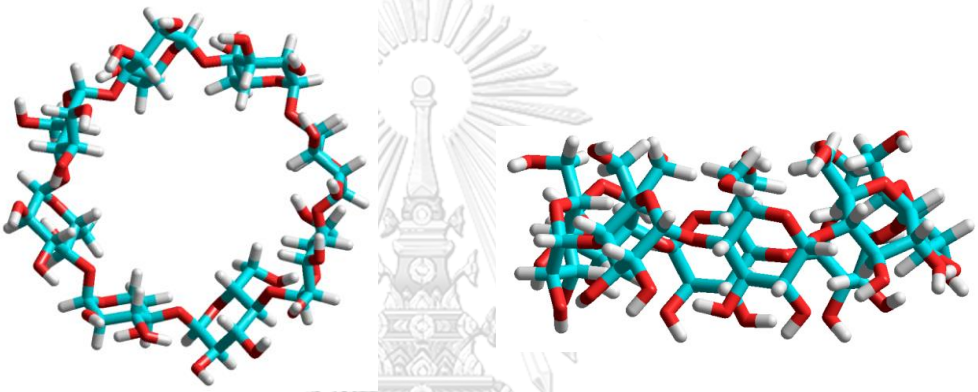

top view side view

Figure 3.1 X-ray crystal structure of the non-modified γ-CD

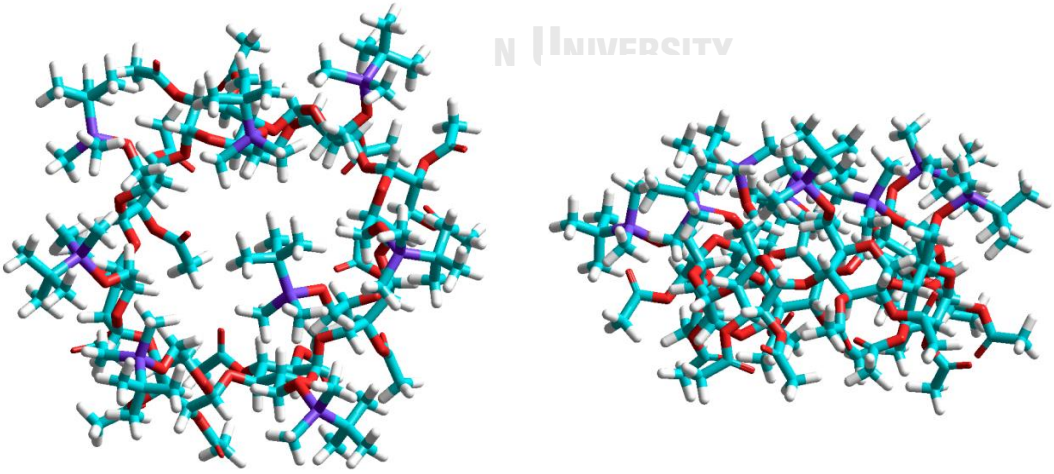

top view side view

Figure 3.2 GSiAc structure optimized with AM1 method

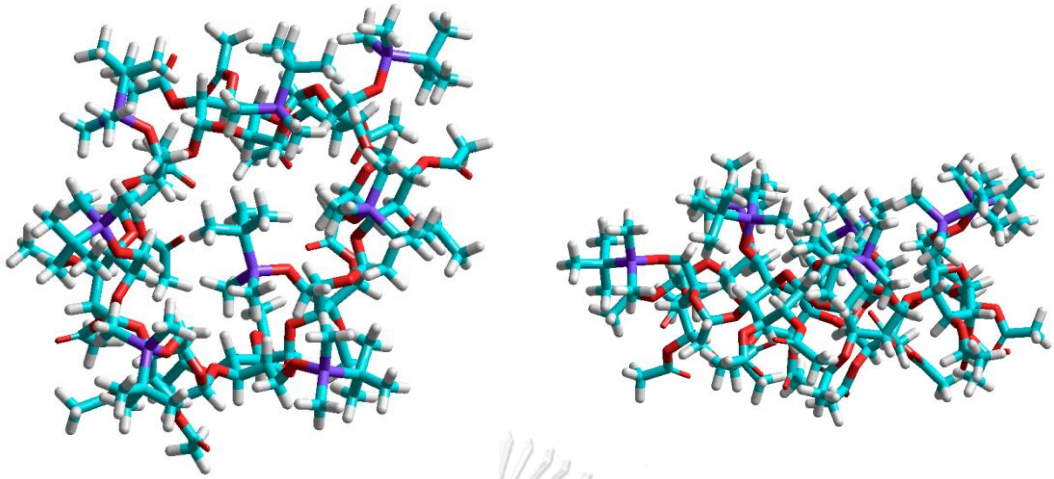

top view side view

Figure 3.3 GSiAc structure optimized with PM7 method

3.3.2 Alcohol structures

The structures of both *R*- and *S*-forms of each alcohols were constructed using HyperChem software and were geometrically optimized at HF/3-21G level of theory. The optimized structures were then used for molecular docking calculations and QSPR study. The optimized structures of (*R*)- and (*S*)-1-phenylethanol are shown in Figure 3.4.

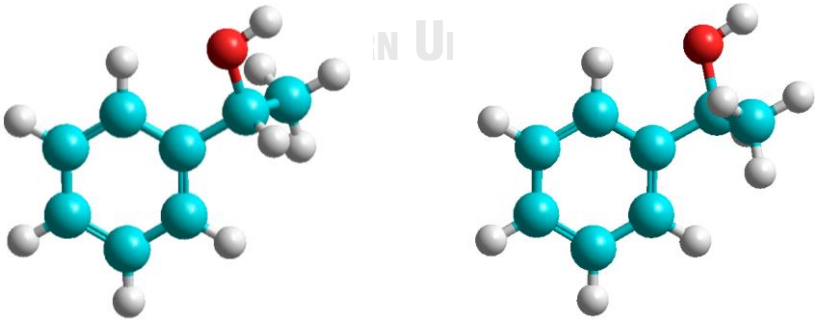

Figure 3.4 HF/3-21G optimized structures of 1-phenylethanol with *R*-configuration (left) and *S*-configuration (right).

3.3.3 Molecular docking calculations

Molecular docking calculations between GSiAc and each alcohol were carried out using the AutoDock 4.2 [51] together with the AutoDockTools (ADT) [52], which was used to prepare input files. For GSiAc, both AM1 and PM7 optimized structures were used. For alcohols, the HF/3-21G optimized structures were used and the atomic charges were calculated with PM7 method.

The grid map of dimension 60 x 60 x 60 $Å^3$ with a grid spacing of 0.375 Å was placed covering the GSiAc molecule. 100 docking runs were performed for each guest molecule. The run was terminated if either 2,500,000 numbers of energy evaluations or 270,000 numbers of generations was reached.

Since the genetic algorithm (GA) is based on random movements, the final docked configuration depends on the starting configuration. In order to avoid any bias and to generate as many final docked configurations as possible, the starting configuration was assigned in random manner for each docking calculation. A cluster analysis was used to categorize all 100 docked configurations into groups. Configurations with root-mean-square-deviation (rmsd) values of less than 2 Å were group together. In each group, the lowest energy configuration was selected as the representative of that group. The % frequency was used to represent number of members (configurations) in each group. Our attention was focused on the group with the highest % frequency (the dominating configuration) and average of 100 docked configurations.

3.3.4 Binding energy calculations

GSiAc-alcohol complex structure of a cluster with the highest % frequency from docking calculation was used as an initial complex structure for the calculation of binding energy at the PM7 level using MOPAC2016 software. This binding energy was used to predict the enantioselectivity.

3.3.5 MD simulation

MD simulation were performed using the HyperChem software. Kinetic energy (E_k), potential energy (E_p) and total energy (E) of each pair of enantiomers were considered. MM+ force field was used in this simulation, set up time to simulation was 100 picoseconds and periodic box size was 50x50x50 $Å^3$. All solvent (water) molecules were deleted in the periodic box.

3.3.6 QSPR Study

Alcohols properties calculation

One hundred thirty-seven structural properties of alcohols were calculated by Materials Studio software (BIOVIA). These properties were then used to find relationship.

Finding QSPR models

QSPR models were created using statistical method to find the relationship between the calculated structural properties and the elution temperature from the experiment. Partial least square (PLS), multiple linear regression (MLR) and genetic function approximation (GFA) methods were used to create QSPR model.

CHAPTER IV
Results and discussions

4.1 Enantiomeric separation of chiral alcohols by GC

4.1.1 Enantiomeric separation by temperature program

Gas chromatographic enantiomeric separation for 55 alcohols was studied using the acetylated γ-CD, GSiAc, as a chiral stationary phase. All 55 alcohols were individually analyzed by a temperature program starting from 40 °C to 220 °C at a rate of 3.3 °C/min. The elution temperatures for all eluted peaks and the resolution between the peak pair were calculated and will be further used in molecular modeling.

Table 4.1 Retention times, elution temperatures and resolution of 55 alcohols

analyte	$t_{R,1}$ (min)	$t_{R,2}$ (min)	$w_{h,1}$ (min)	$w_{h,2}$ (min)	elution $temp_1$ (ºC)	elution $temp_2$ (ºC)	Rs
1	18.23	18.36	0.0520	0.0563	100.15	100.57	1.38
2F	19.33	-	0.0597	-	103.79	-	-
3F	20.43	20.69	0.0546	0.0554	107.43	108.27	2.74
4F	19.83	20.61	0.0553	0.0536	105.45	108.02	8.43
2Cl	26.10	26.19	0.0504	0.0539	126.12	126.44	1.08
3Cl	27.45	27.70	0.0562	0.0568	130.57	131.40	2.60
4Cl	27.89	28.61	0.0580	0.0574	132.02	134.42	7.39
2Br	27.35	27.54	0.0547	0.0564	130.26	130.87	1.97
3Br	29.15	29.35	0.0583	0.0577	136.19	136.85	2.05
4Br	30.99	31.62	0.0622	0.0546	142.28	144.34	6.30
2Me	21.79	22.58	0.0547	0.0519	111.90	114.51	8.73
3Me	19.81	20.25	0.0564	0.0525	105.38	106.82	4.72
4Me	20.54	21.12	0.0527	0.0534	107.77	109.69	6.48
2CF3	18.81	20.42	0.0546	0.0526	102.09	107.40	17.68
3CF3	21.96	-	0.0777	-	112.47	-	-
4CF3	21.98	22.61	0.0526	0.0525	112.54	114.60	7.00

analyte	$t_{R,1}$ (min)	$t_{R,2}$ (min)	$w_{h,1}$ (min)	$w_{h,2}$ (min)	elution $temp_1$ (ºC)	elution $temp_2$ (ºC)	Rs
4Et	22.84	23.23	0.0549	0.0550	115.36	116.66	4.22
4Bu	28.66	28.96	0.0582	0.0583	134.56	135.55	3.03
4tBu	25.80	25.99	0.0587	0.0607	125.13	125.75	1.86
4Phe	41.31	41.59	0.0617	0.0617	176.33	177.24	2.63
24Me	23.91	24.72	0.0564	0.0552	118.90	121.56	8.51
25Me	23.77	23.92	0.0583	0.0545	118.44	118.95	1.59
34Me	23.00	23.16	0.0617	0.0590	115.89	116.43	1.62
2	36.99	37.26	0.0624	0.0626	162.05	162.96	2.61
3	36.21	-	0.0620	-	159.48	-	-
4	27.64	-	0.0584	-	131.22	-	-
5	29.71	-	0.0705	-	138.03	-	-
6	24.19	24.25	0.0503	0.0534	119.83	120.03	0.68
7	20.99	21.95	0.0514	0.0506	109.25	112.43	11.11
8	23.78	24.42	0.0536	0.0511	118.48	120.58	7.14
9	22.26	23.63	0.0540	0.0532	113.45	117.99	15.11
10	23.60	23.99	0.0548	0.0553	117.86	119.18	4.25
11	39.16	39.33	0.0641	0.0635	169.23	169.80	1.60
12	23.94	24.83	0.0501	0.0514	119.00	121.95	10.37
13	18.75	19.11	0.0551	0.0545	101.87	103.05	3.86
2MeBen	39.87	40.11	0.0646	0.0618	171.58	172.36	2.20
3MeBen	39.86	-	0.0677	-	171.52	-	-
4MeBen	39.47	39.71	0.0596	0.0583	170.25	171.04	2.38
4OMeBen	44.39	44.48	0.0574	0.0644	186.48	186.77	0.87
4FBen	37.90	38.03	0.0569	0.0588	165.06	165.50	1.34
4ClBen	43.50	43.63	0.0641	0.0628	183.55	183.99	1.22
4BrBen	46.16	46.27	0.0678	0.0626	192.33	192.70	1.02
2but	2.05	2.08	0.0231	0.0288	46.77	46.86	0.61
2pen	3.63	3.69	0.0336	0.0396	51.98	52.17	0.95

analyte	$t_{R,1}$ (min)	$t_{R,2}$ (min)	$w_{h,1}$ (min)	$w_{h,2}$ (min)	elution $temp_1$ (ºC)	elution $temp_2$ (ºC)	Rs
2hex	5.72	5.88	0.0436	0.0448	58.88	59.41	2.16
3hex	5.93	6.03	0.0429	0.0453	59.56	59.89	1.32
2hep	8.54	8.59	0.0445	0.0479	68.18	68.36	0.71
3hep	8.65	-	0.0846	-	68.53	-	-
2oc	11.90	11.98	0.0487	0.0530	79.28	79.52	0.82
3oc	10.86	10.94	0.0496	0.0509	75.83	76.10	0.96
4oc	10.85	10.97	0.0495	0.0497	75.79	76.20	1.48
2non	14.37	-	0.0696	-	87.43	-	-
3non	14.33	-	0.0598	-	87.27	-	-
2dec	17.88	-	0.0698	-	99.00	-	-
2undec	21.35	-	0.0624	-	110.44	-	-

From 55 alcohols of various structures, 44 alcohols could be separated into their enantiomers. Eleven alcohols, including **3hep, 2non, 3non, 2dec, 2undec, 2F, 3CF3, 3MeBen, 3, 4** and **5**, could not be separated into their enantiomers under the temperature program condition using the GSiAc stationary phase. The 11 non-separable alcohols include aliphatic and aromatic structures. Among 13 aliphatic alcohols used in this study, **2hex** was the only aliphatic alcohol that could be completely separated into their enantiomers, with the resolution of 2.16. Other 7 aliphatic alcohols showed some degree of separation, but complete resolutions of two enantiomeric peaks were not achieved. Five aliphatic alcohols could not be separated.

Among 44 separable alcohols, 30 alcohols could be completely separated into their enantiomers under the temperature program with resolutions of 1.5 or higher. Most of them are alcohols with one aromatic ring with substitution(s) on the aromatic ring.

4.1.2 Enantiomeric separation by isothermal condition

Based on the results from temperature program, 25 alcohols were selected to study under isothermal condition. These alcohols were 1-phenylethanol analogs with substitution on the aromatic ring or substitution at the stereogenic center. They are **1**, **7**, **8**, **9**, **10**, **11**, **2F**, **3F**, **4F**, **2Cl**, **3Cl**, **4Cl**, **2Br**, **3Br**, **4Br**, **2Me**, **3Me**, **4Me**, **2CF3**, **3CF3**, **4CF3**, **4Et**, **4Bu**, **4tBu** and **4Phe**. Each alcohol was analyzed isothermally every 10 °C interval at 6-8 different temperatures. Retention factor (k'), enantioselectivity (α), and resolution (Rs) were calculated at each temperature. Retention factors of

enantiomers were studied as a function of temperature according to van't Hoff equation [31, 35].

$$\ln k' = -\frac{\Delta H}{RT} + \frac{\Delta S}{R} - \ln \beta$$

Plots of ln k' versus 1/T of each enantiomer for all 25 alcohols showed linear relationship with correlation coefficient (R^2) greater than 0.9982. Figure 4.1 showed plots of ln k′ versus 1/T of the more retained enantiomers of all 25 alcohols. For all analytes, the retention factors increased as the temperature decreased. At the same column temperature, 1-phenylethanol (**1**) was the least retained alcohol on this column. Alcohols with larger alkyl or phenyl group showed higher retention factors. Alcohols **4Phe** and **11**, with the largest substituent (phenyl group) on the aromatic ring and on the side chain, were the two longest retained analytes in this study.

Twenty-five alcohols used in this study could be separated into their enantiomers using the acetylated GSiAc column. Plots of ln α versus 1/T of all 25 analytes were compared in Figure 4.2. The difference in enthalpy change (ΔΔH) and the difference in entropy change (ΔΔS) for the enantiomeric separation could be obtained. Large difference in thermodynamic terms indicated that the separation could be easily improved with a decrease in temperature according to equation below.

$$\ln \alpha = \frac{-\Delta(\Delta H)}{RT} + \frac{\Delta(\Delta S)}{R}$$

For most analytes, enantioselectivities increased as the column temperature decreased, except for **2F**: enantioselectivities were slightly affected by column temperature and were decreased in the 110-80 °C range. Enthalpy differences (-ΔΔH) for the enantiomeric separations of **1** and its 24 analogs were compared in Figure 4.3. Using 1-phenylethanol (**1**) as a reference analyte, the influence of column temperature on enantioselectivity of analytes with different type and position of substituent was examined.

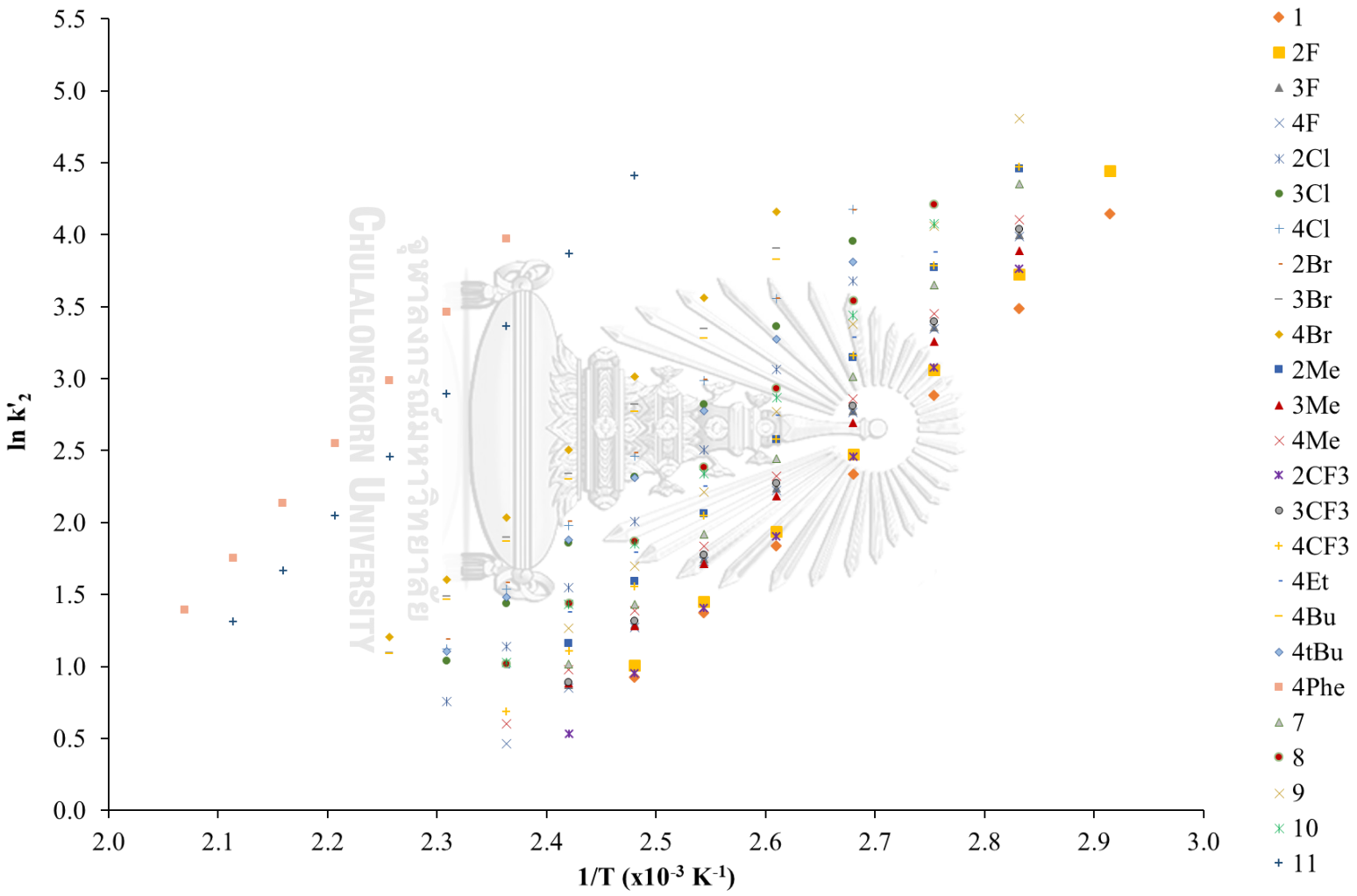

Figure 4.1 Plots of ln k' versus 1/T of the more retained enantiomers of 25 alcohols

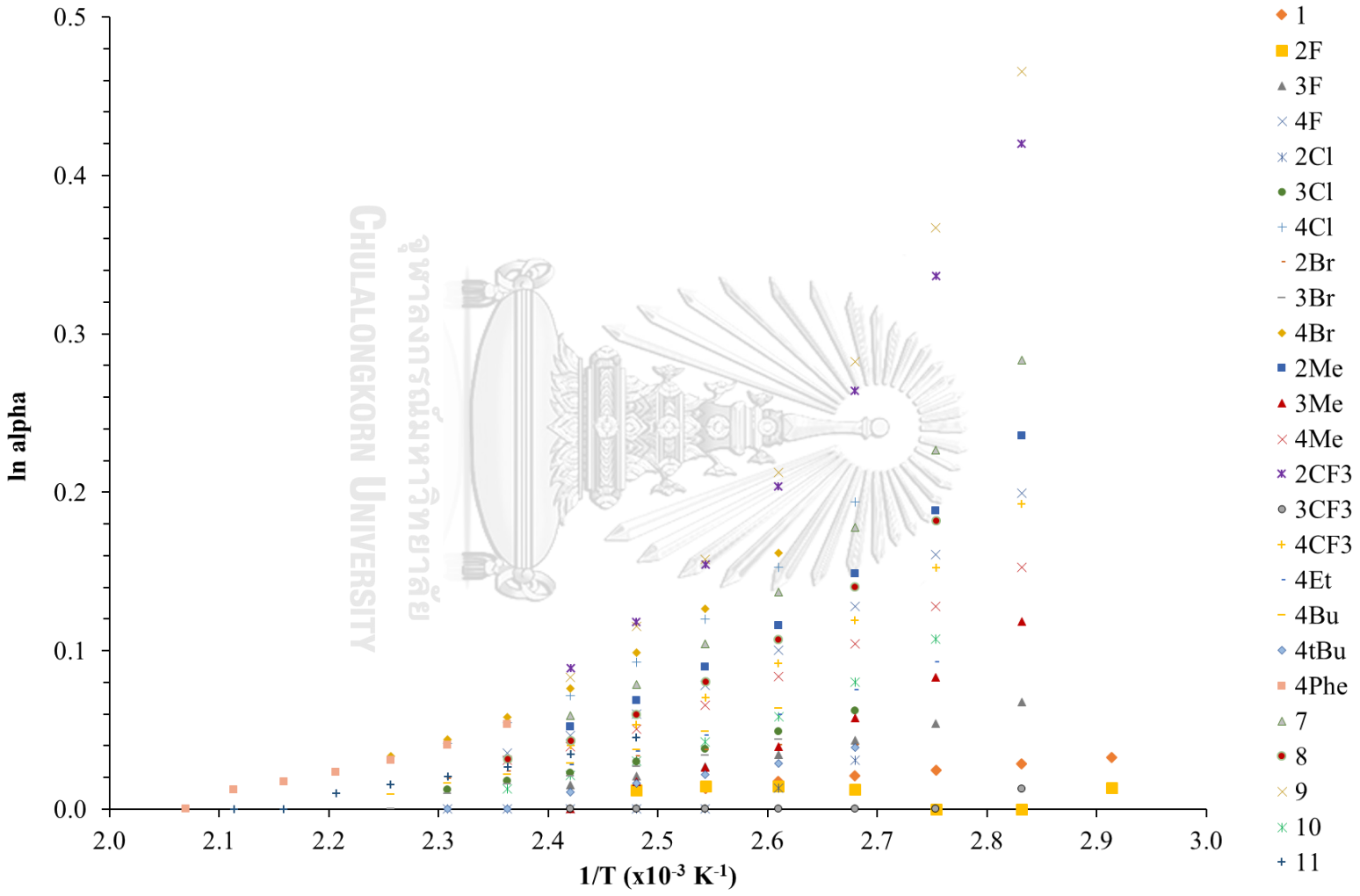

Figure 4.2 Plots of ln α versus 1/T of 25 alcohols

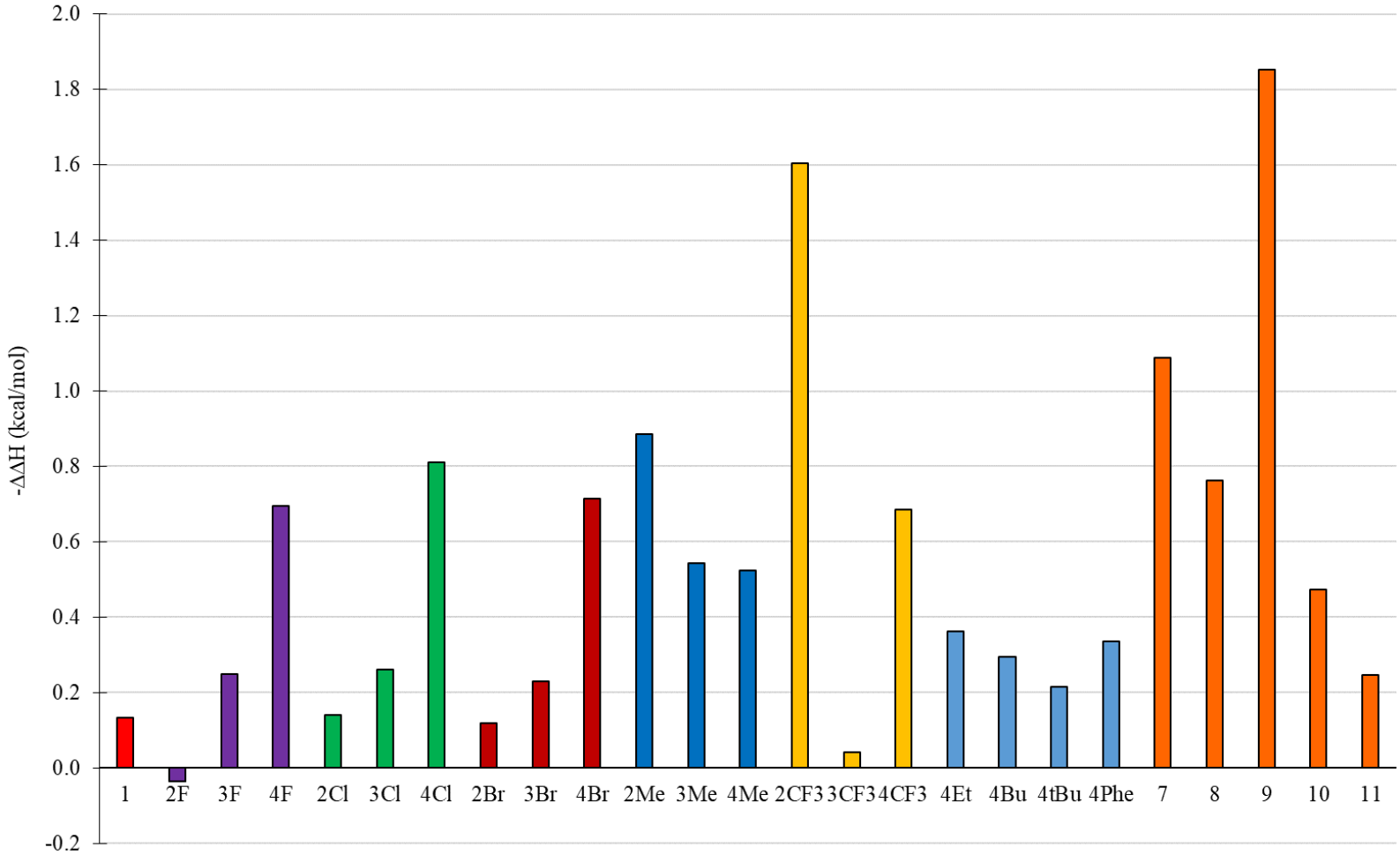

Figure 4.3 Enthalpy difference (–ΔΔH, kcal/mol) of 25 alcohols

- **Effect of type of substituent at the *para*-position of the aromatic ring**

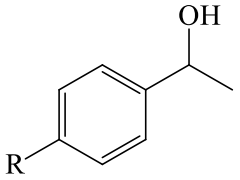

R = -H, -F, -Cl, -Br, -Me, $-CF_3$, -Et, -Bu, -*t*Bu, -Phe

The effect of type of substituent at the *para*-position of the aromatic ring of 1-phenylethanol was examined. These alcohols include **4F**, **4Cl**, **4Br**, **4Me**, **4CF3**, **4Et**, **4Bu**, **4tBu** and **4Phe**.

All nine 1-phenylethanols with *para*-substitution on the aromatic ring showed sharper slopes of ln α versus 1/T plots compared to 1-phenylethanol (**1**) (Figure 4.2). Alcohols with electron withdrawing group, e.g. halogen (**4F**, **4Cl** and **4Br**) or trifluoromethyl (**4CF3**), showed sharper slopes of ln α versus 1/T plots than those of alcohols with alkyl group (**4Me**, **4Et**, **4Bu**, **4tBu**) or phenyl group (**4Phe**). This indicated that the enantioselectivities of alcohols with sharper slopes could be easily improved with the decrease in column temperature. The slopes of ln α versus 1/T plots of alcohols in this group were in the order of **4Cl** > **4Br** > **4F** > **4CF3** > **4Me** > **4Et** > **4Phe** > **4Bu** > **4tBu** > **1**. In addition, the enantioselectivities of analytes **4F**, **4Cl**, **4Br**, **4Me**, **4CF3**, **4Et** and **4Bu** were higher than that of analyte **1** at the same temperature. Thus, complete enantiomeric separations of these analytes could be achieved at higher column temperature and probably with shorter analysis time than analyte **1**. Alcohols **4tBu** and **4Phe**, with bulky *tert*-butyl group or large phenyl group at the *para*-position of the aromatic ring, gave lower slopes of ln α versus 1/T plots than most alcohols in this group. The enantiomeric separations of **4Me**, **4Et**, **4Bu** and **4tBu** were compared at 140 °C (Figure 4.4). Enantiomeric separations of **4Me** and **4Et** were better achieved in shorter analysis time compared to **4Bu** and **4tBu**. Although isomer **4tBu** was less retained, enantiomers of isomer **4Bu** were better separated.

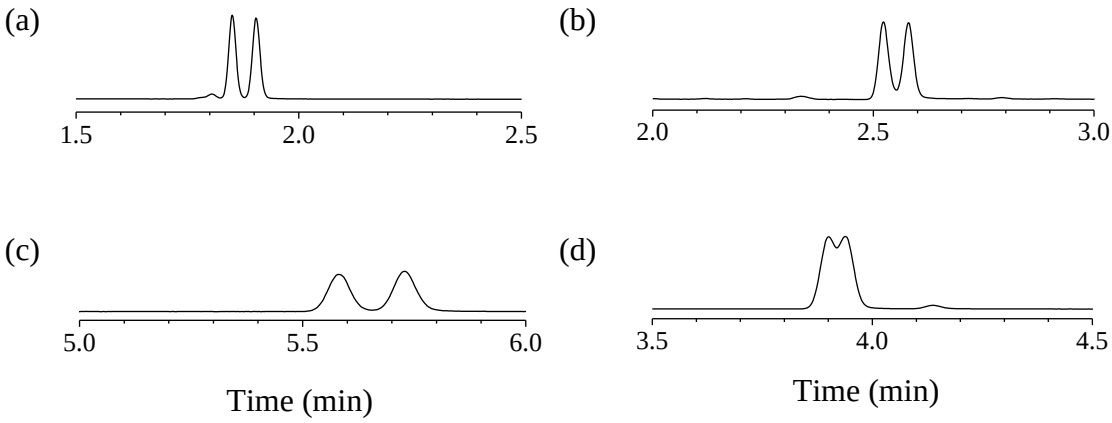

Figure 4.4 Enantiomeric separation of (a) **4Me** (b) **4Et** (c) **4Bu** and (d) **4tBu** at 140 °C

- **Effect of type and position of substituent on the aromatic ring**

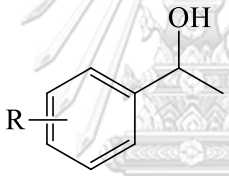

R = -H, -F, -Cl, -Br, -Me, -CF_3

Effects of type and position of substituent on the aromatic ring of 1-phenylethanol on the enantioseparation were studied as a function of temperature. 1-Phenylethanol (**1**) was used as a reference compound. Other 15 alcohols were 1-phenylethanols with mono-substitution of fluoro (**2F**, **3F**, **4F**), chloro (**2Cl**, **3Cl**, **4Cl**), bromo (**2Br**, **3Br**, **4Br**), trifluoromethyl (**2CF3**, **3CF3**, **4CF3**) and methyl (**2Me**, **3Me**, **4Me**) groups at *ortho*-, *meta*- and *para*-positions.

Most alcohols showed sharper slopes of ln α versus 1/T plots (corresponded to higher −ΔΔH values) compared to alcohol **1**, except for three alcohols: **2F**, **2Br** and **3CF3** (Figure 4.3). The −ΔΔH values depended on the type and position of substitution. The enantioselectivities of alcohols with sharper slopes or higher −ΔΔH values could be easily improved with the decrease in column temperature. For all halogen-substituted alcohols, the −ΔΔH values were in the order of *para* > *meta* > *ortho*. The enantiomeric separation of 2Cl, 3Cl and 4Cl were compared at 140 °C (Figure 4.5). However, for larger sized, methyl- or trifluoromethyl-substituted alcohols, the −ΔΔH values were highest at *ortho*-position. Among 15 substituted alcohols, trifluoromethyl-substituted 1-phenylethanol at *ortho*-position (**2CF3**) showed the highest −ΔΔH value.

Interestingly, **2F** showed small positive ΔΔH value (Figure 4.3). Alcohol **2F** was analyzed isothermally in the 130-70 °C range. At 130 °C, enantioselectivity was 1.012. The decrease in column temperature to 110 °C slightly improved its enantioselectivity to 1.015. However, further decrease in column temperature to 90 °C diminished its enantioselectivity and only one peak was observed (no enantioseparation). Enantioselectivity was detected again at 70 °C. It was likely that there was a reversal in elution order of the two enantiomers of **2F** in the temperature range studied. For **2F**, complete enantioseparation could not be achieved.

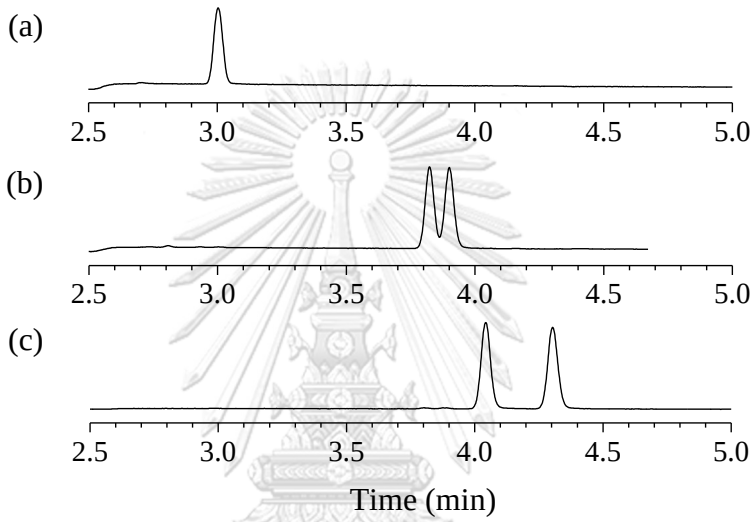

Figure 4.5 Enantiomeric separation of alcohols (a) **2Cl** (b) **3Cl** and (c) **4Cl** at 140 °C

- **Effect of type of substituent at the stereogenic center**

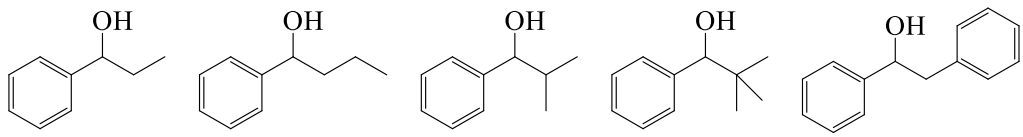

7 **8** **9** **10** **11**

The influence of column temperature on enantioselectivity of 1-phenylethanols with different type of substituent at the stereogenic center was also studied. These analytes are 1-phenylethanols with alkyl or phenyl group substituted at the stereogenic center (alcohols **7**, **8**, **9**, **10** and **11**). When the methyl group at the stereogenic center of **1** was replaced by a larger alkyl or phenyl group (alcohols **7-11**), the enantioselectivities

of these alcohols improved as seen from the sharper slopes of ln α versus 1/T plots (Figure 4.2) or higher −ΔΔH values (Figure 4.3).

Comparing the ln α versus 1/T plots of alcohols **7-11** (Figure 4.2), it can be seen that alcohols with smaller alkyl substituents (**7-9**) showed sharper slopes than those of alcohols with bulky alkyl group or large phenyl group (**10-11**), similar to the results obtained from the type of substituent at the *para*-position of the aromatic ring. The enantiomeric separations of alcohols **7-9** and **10** were compared at 140 °C (Figure 4.6). Interestingly, the *iso*-propyl group substituted at the stereogenic center (**9**) can greatly improve enantioseparation. The enantiomeric separations of small or medium size substituted isomers with different position of substituent were also compared; e.g. **7** vs. **4Me** and (**8** and **9**) vs. **4Et**. It was found that alcohols with the substituent at the stereogenic center seem to provide better enantioselectivity than those with the substituent at the *para*-position of the aromatic ring. At the same column temperature, the enantioselectivities of **7** > **4Me** and of (**8** and **9**) > **4Et**.

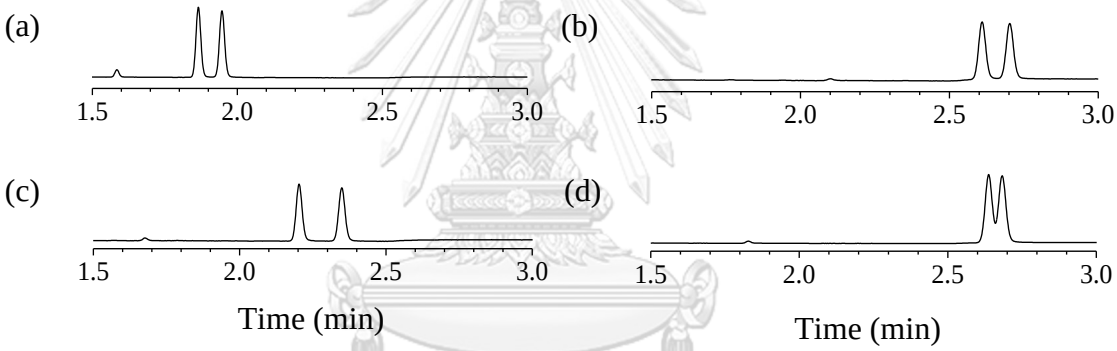

Figure 4.6 Enantiomeric separation of alcohols (a) **7** (b) **8** (c) **9** and (d) **10** at 140 °C

4.1.3 Retention factor at complete baseline separation

As seen from Figures 4.1-4.2, the decrease in column temperature resulted in the increase in retention factor as well as enantioselectivity. Based on the isothermal study (section 4.1.2), the isothermal temperature and the retention factor for each alcohol giving a complete baseline separation of enantiomers (Rs = 1.5) were determined. From 25 alcohols studied under isothermal condition in section 4.1.2, complete baseline separation of enantiomers of two alcohols, **2F** and **3CF3**, could not be obtained. The retention factors of the more retained enantiomers (k'_2) of 23 separable alcohols (except **2F** and **3CF3**) were compared in Figure 4.7.

From Figure 4.7, enantiomers of 1-phenylethanol (**1**) could be completely separated with the retention factor of the more retained enantiomer of 20.09 (retention time of 11.199 minutes). Using alcohol **1** as a reference, only 3 alcohols were separated into their enantiomers with longer analysis time than **1** (higher k'_2 values than **1**). They

were **2Cl**, **4tBu** and **11**. Fortunately, enantiomers of most alcohols could be completely separated in shorter analysis time (lower k'_2 values than alcohol **1**) using the GSiAc stationary phase. This suggested that substitution on 1-phenylethanol, either on the aromatic ring or at the stereogenic center, tended to improve enantioselectivity. Alcohols with small *para*-substitution on the aromatic ring (**4F, 4Cl**, **4Br**, **4Me**, **4Et** and **4CF3**) could be baseline separated with very short retention ($k'_2 < 5$). **2Me** and **2CF3** could be baseline separated with short retention as well. Alcohols with small alkyl group substituted at the stereogenic center (**7**, **8** and **9**) also showed short retention ($k'_2 < 5$) for complete separation of their enantiomers. Among 25 analytes in this study, enantiomers of 2-methyl-1-phenyl-1-propanol (**9**) could be baseline separated with the shortest analysis time ($k'_2 = 1.72$ and retention time of 1.419 minutes). These results indicated the importance of both type and position of substituent towards enantioseparation.

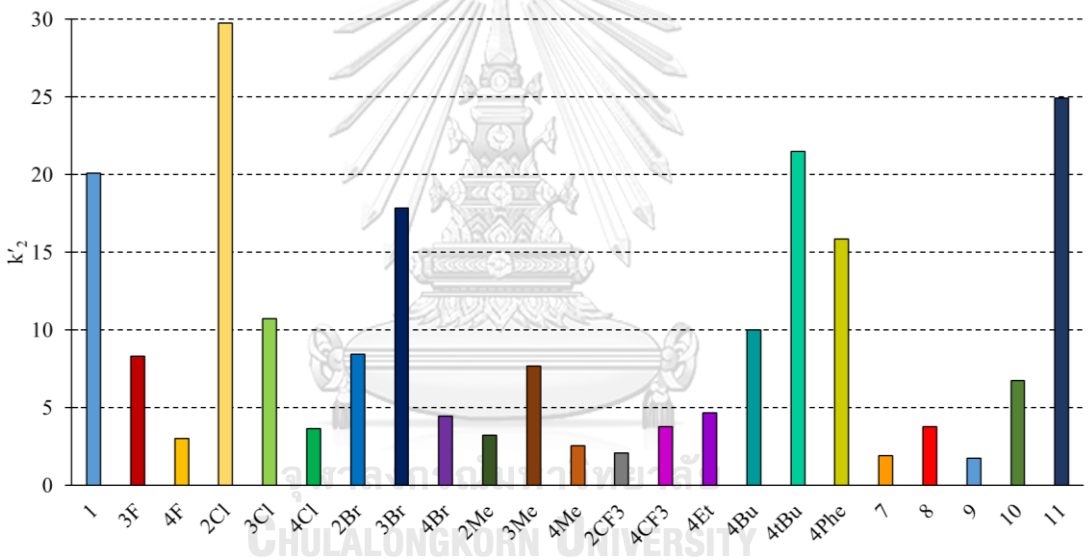

Figure 4.7 Retention factors of the more retained enantiomers (k'_2) at baseline separation

4.2 Molecular modeling

In this research works, several molecular modeling techniques were employed (Figure 4.8). First, QSPR technique was used to figure out whether the difference in elution temperature of each pair of enantiomers (which indicates the successful of enantioseparation) could be predicted from difference in properties of each pair of enantiomers (section 4.2.3). Second, molecular docking calculations were applied to examine whether each pair of enantiomers has different interaction with GSiAc and whether this difference is related with enantioselectivity (section 4.2.1). Third, molecular dynamics (MD) simulations were introduced for 5 enantiomeric pairs of

compounds to include flexibility of both host and guest molecules into the calculations of host-guest interaction. Forth, QSPR technique was reconsidered but this time two models were investigated, one for more retained enantiomers and another for less retained enantiomers, to predict elution temperature (section 4.2.3).

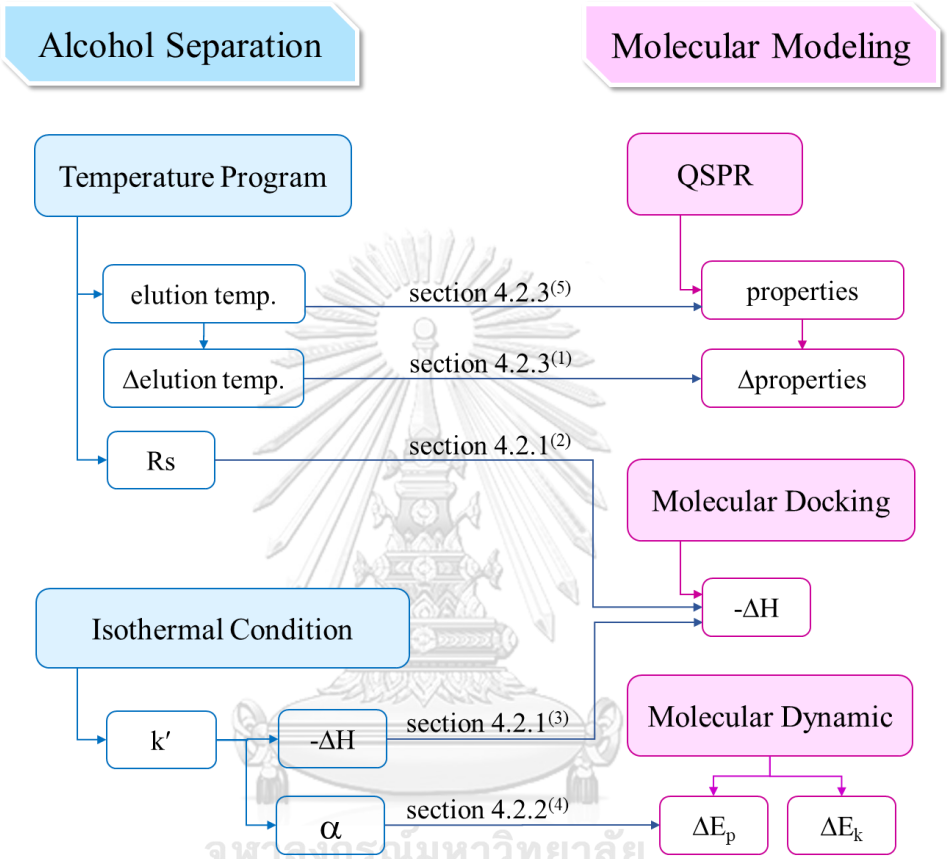

Figure 4.8 Flowchart showing the procedure to find the relationship between chromatographic parameters and molecular modeling parameters (number in parenthesis indicates the sequence of the work in this research).

4.2.1 Molecular docking

For GSiAc molecule, 4 different geometries were used including AM1 and PM7 optimized structures, each with two different conformations - substituent inside and outside the cavity. In addition, the unmodified γ-cyclodextrin was also used for comparison purpose. The results showed that asymmetric PM7 geometry gave the best predictive value.

The docking results between alcohols and PM7 geometry of GSiAc with substituent inside the cavity (Figure 4.10) were summarized in Table 4.2. In this study,

the binding energies were taken from the most probable configuration, a cluster with the highest % frequency.

Table 4.2 The docking results of alcohols and GSiAc

analyte		$\Delta H^{(a)}$ (kcal/mol)	% frequency	$-\Delta(\Delta H)^{(b)}$ (kcal/mol)	$\Delta H_{mean}^{(c)}$	$-\Delta(\Delta H_{mean})^{(d)}$
1	*R*	-2.48	72	0.04	-2.4213	0.0317
	S	-2.52	69		-2.4530	
2	*R*	-3.33	51	0.09	-3.1718	0.0496
	S	-3.24	53		-3.1222	
3	*R*	-3.04	34	0.26	-2.8310	0.0238
	S	-2.78	58		-2.8548	
4	*R*	-2.97	72	0.21	-2.9085	0.1645
	S	-2.76	64		-2.7440	
5	*R*	-2.97	89	0.37	-2.9464	0.2393
	S	-2.60	41		-2.7071	
6	*R*	-2.75	50	0.02	-2.7554	0.0507
	S	-2.77	74		-2.7047	
7	*R*	-2.48	59	0.05	-2.3561	0.0182
	S	-2.43	65		-2.3743	
8	*R*	-2.50	39	0.15	-2.2379	0.0573
	S	-2.35	24		-2.1806	
9	*R*	-2.56	37	0.13	-2.3990	0.0416
	S	-2.43	37		-2.3574	
10	*R*	-2.18	27	0.05	-2.3393	0.0607
	S	-2.23	51		-2.2786	
11	*R*	-2.83	48	0.34	-2.7181	0.0352
	S	-2.49	40		-2.6829	
12	*R*	-2.11	47	0.18	-1.9722	0.1155
	S	-2.29	46		-2.0877	
13	*R*	-2.56	50	0.18	-2.3963	0.1015
	S	-2.38	50		-2.2948	
2F	*R*	-2.44	53	0.01	-2.3612	0.0026
	S	-2.45	72		-2.3638	

analyte		$\Delta H^{(a)}$ (kcal/mol)	% frequency	$-\Delta(\Delta H)^{(b)}$ (kcal/mol)	$\Delta H_{mean}^{(c)}$	$-\Delta(\Delta H_{mean})^{(d)}$
3F	*R*	-2.45	79	0.01	-2.4014	0.0129
	S	-2.44	76		-2.3885	
4F	*R*	-2.42	84	0.02	-2.3754	0.0292
	S	-2.44	86		-2.4046	
2Cl	*R*	-2.62	43	0	-2.3789	0.1011
	S	-2.62	47		-2.4800	
3Cl	*R*	-2.66	44	0.01	-2.5779	0.0030
	S	-2.65	52		-2.5749	
4Cl	*R*	-2.69	91	0.02	-2.6584	0.0109
	S	-2.71	88		-2.6693	
2Br	*R*	-2.26	26	0.2	-2.4496	0.1129
	S	-2.46	40		-2.5625	
3Br	*R*	-2.80	36	0	-2.7244	0.0240
	S	-2.80	32		-2.7004	
4Br	*R*	-2.79	96	0.03	-2.7759	0.0180
	S	-2.82	93		-2.7939	
2Me	*R*	-2.54	53	0.06	-2.3780	0.0957
	S	-2.60	56		-2.4737	
3Me	*R*	-2.66	50	0.04	-2.5762	0.0065
	S	-2.62	61		-2.5697	
4Me	*R*	-2.62	89	0.03	-2.5857	0.0372
	S	-2.65	90		-2.6229	
2CF3	*R*	-2.26	35	0	-1.9578	0.1359
	S	-2.26	43		-2.0937	
3CF3	*R*	-2.25	45	0.02	-2.1666	0.0080
	S	-2.23	52		-2.1746	
4CF3	*R*	-2.32	89	0.01	-2.2826	0.0246
	S	-2.33	93		-2.3072	
4Et	*R*	-2.61	89	0.01	-2.5688	0.0042
	S	-2.62	87		-2.5730	
4Bu	*R*	-2.52	67	0.06	-2.4244	0.0397
	S	-2.58	59		-2.4641	
4tBu	*R*	-2.88	75	0.02	-2.8311	0.0242

analyte		$\Delta H^{(a)}$ (kcal/mol)	% frequency	$-\Delta(\Delta H)^{(b)}$ (kcal/mol)	$\Delta H_{mean}^{(c)}$	$-\Delta(\Delta H_{mean})^{(d)}$
	S	-2.86	83		-2.8069	
4Phe	*R*	-2.93	53	0.01	-2.9783	0.0234
	S	-2.94	27		-3.0017	
24Me	*R*	-2.26	56	0.42	-2.4306	0.0890
	S	-2.68	47		-2.5196	
25Me	*R*	-2.51	54	0.14	-2.6070	0.0299
	S	-2.65	52		-2.6369	
34Me	*R*	-2.81	64	0.05	-2.7314	0.0777
	S	-2.76	56		-2.6537	
2MeBen	*R*	-2.77	44	0.02	-2.8267	0.0035
	S	-2.79	79		-2.8302	
3MeBen	*R*	-2.98	83	0.01	-2.9799	0.0340
	S	-2.97	45		-3.0139	
4MeBen	*R*	-2.96	70	0.03	-2.9934	0.0555
	S	-2.93	64		-2.9379	
4OMeBen	*R*	-2.56	46	0	-2.5882	0.0215
	S	-2.56	45		-2.5667	
4BrBen	*R*	-3.22	87	0.01	-3.2294	0.0348
	S	-3.21	84		-3.1946	
4ClBen	*R*	-3.02	79	0	-3.0464	0.0426
	S	-3.02	59		-3.0038	
4FBen	*R*	-2.57	29	0.2	-2.6830	0.0252
	S	-2.77	35		-2.7082	
2but	*R*	-1.56	35	0	-1.6429	0.0733
	S	-1.56	34		-1.7162	
2pen	*R*	-1.65	38	0.02	-1.6360	0.0067
	S	-1.63	41		-1.6427	
2hex	*R*	-1.76	41	0.08	-1.6959	0.0452
	S	-1.68	48		-1.6507	
3hex	*R*	-1.60	45	0	-1.6172	0.0075
	S	-1.60	41		-1.6097	
2hep	*R*	-1.71	51	0.07	-1.6432	0.0222
	S	-1.64	44		-1.6210	

analyte		$\Delta H^{(a)}$ (kcal/mol)	% frequency	$-\Delta(\Delta H)^{(b)}$ (kcal/mol)	$\Delta H_{mean}^{(c)}$	$-\Delta(\Delta H_{mean})^{(d)}$
3hep	*R*	-1.58	44	0.04	-1.6098	0.0237
	S	-1.54	33		-1.5861	
2oc	*R*	-1.62	38	0.02	-1.5704	0.0391
	S	-1.64	36		-1.6095	
3oc	*R*	-1.63	34	0.01	-1.5782	0.0149
	S	-1.62	37		-1.5633	
4oc	*R*	-1.48	31	0.01	-1.5293	0.0205
	S	-1.47	39		-1.5088	
2non	*R*	-1.56	36	0.01	-1.5353	0.0009
	S	-1.55	43		-1.5344	
3non	*R*	-1.67	25	0.1	-1.5559	0.0121
	S	-1.57	55		-1.5438	
2dec	*R*	-1.56	34	0.02	-1.4559	0.0463
	S	-1.54	43		-1.5022	
2undec	*R*	-1.61	43	0.09	-1.4491	0.0054
	S	-1.52	64		-1.4545	

[a] Mean binding energy of a cluster with the highest %frequency

[b] The mean binding energy difference between (R) and (S) complexes

[c] Average binding energy of all 100 docked configurations

[d] The difference of average binding energy of all 100 docked configurations between (*R*) and (*S*) complexes

From Table 4.2, the $-\Delta(\Delta H)$ values, the difference of interaction energy between the enantiomeric pairs, were considered as an indicator to qualitatively predict whether the enantiomeric separation in the temperature program would be successful or not. If the difference of interaction energies of the enantiomeric pair is high, the substance should be well separated. For this purpose, a criterion value for $-\Delta(\Delta H)$ must be determined first. From the analysis, the value of 0.34 kcal/mol was set as the criterion. Therefore, analytes with $-\Delta(\Delta H)$ value greater than 0.34 could be separated by this stationary phase. On the other hand, when the value is less than 0.34, the analytes could not be separated. Using this criterion, the accuracy for prediction is 81.82% for separable analytes and 9.09% for non-separable analytes. This makes the overall accuracy to be 67.27%.

Considering -Δ(ΔH$_{mean}$) values as an indicator, the criterion was found to be 0.11 kcal/mol. The accuracy for prediction is 100% for separable analytes and 18.18% for non-separable analytes. This gives the overall accuracy of 83.64 %, which is very good. If the criterion was increased to around 0.38-0.40 kcal/mol, the overall prediction accuracy was reduced to 80.00%. However, the prediction accuracy for non-separable analytes was increased to 36.36% and it was 90.91% for separable analytes.

Considering the percentage of accurate prediction, it was found that if accurate prediction of separable analytes was very high, the overall accurate prediction was also high. This is because of inequal numbers of separable and non-separable analytes in this experiment. There are 44 separable analytes from 55 compounds, thereby, the separable compounds are the majority and have higher influence than non-separable compounds. Therefore, new set of compounds was set up. In this new set, the number of separable compounds was reduced to be equal to that of the non-separable compounds (11 analytes). The overall accuracy for prediction of this new set was 68.18%, which is lower than the original set of compounds.

In addition, the enthalpy (-ΔH) obtained from the isothermal condition were compared with -ΔH$_{mean}$ in Figure 4.9. The correlation r^2 value is 0.0424, which means that both values are not correlated.

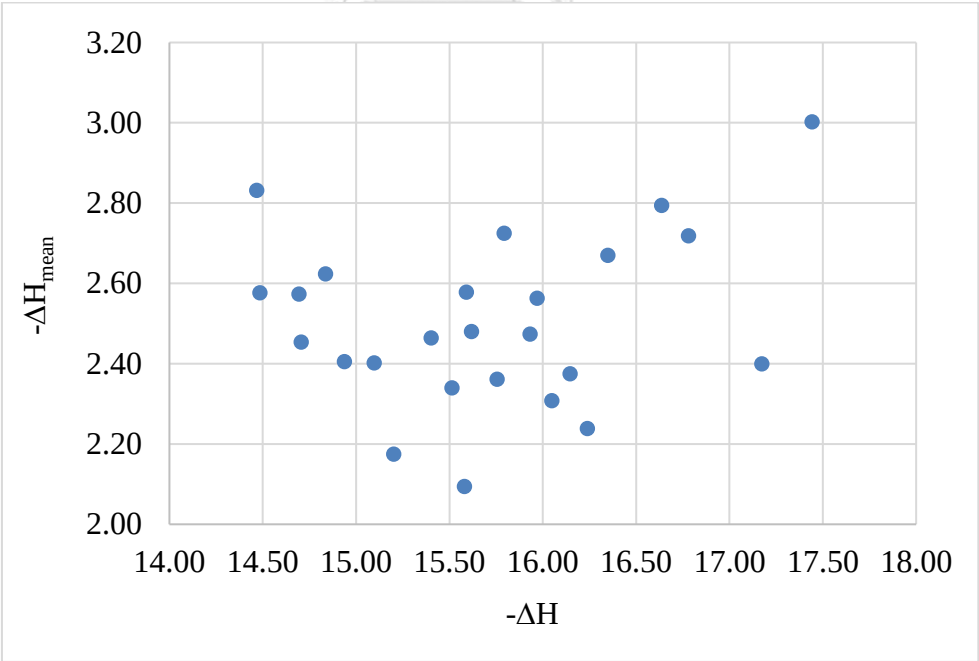

Figure 4.9 Plot of the enthalpy (-ΔH) obtained from the isothermal condition (x-axis) versus average binding energy (-ΔH$_{mean}$) from molecular docking (y-axis)

(a)

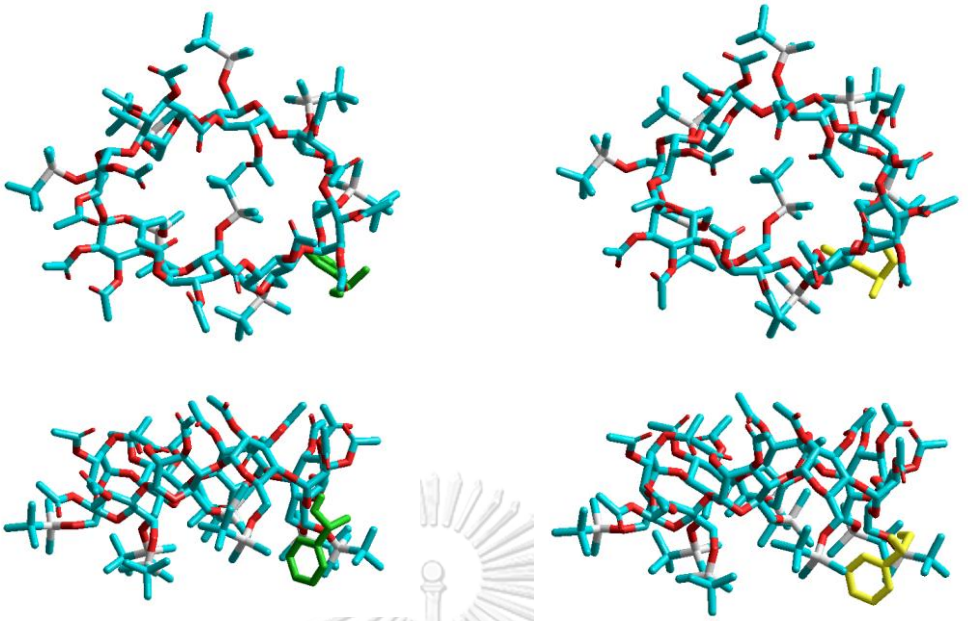

(b)

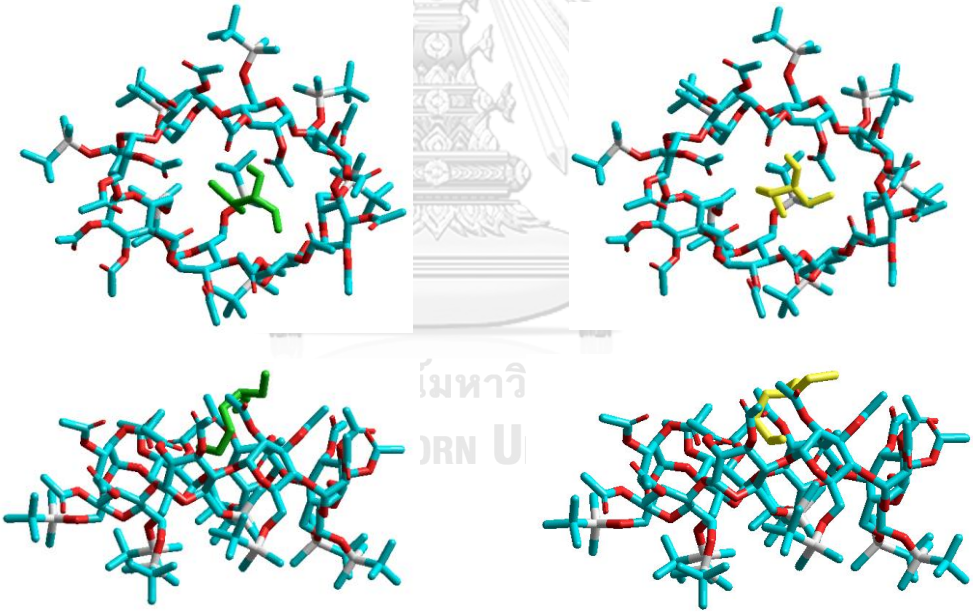

Figure 4.10 The lowest energy complexes between GSiAC and (a) **1** and (b) **3hep** in *R*-form (green) and *S*-form (yellow) in both top and side views.

4.2.2 MD simulation

Although the prediction using information from docking results, $-\Delta(\Delta H_{mean})$, in the previous section was very good (with the overall accuracy of 83.64 %), it is still not satisfying for non-separable compounds. This is possibly because GSiAc was treated as rigid molecule during the docking calculation, the obtained binding energy may not correspond to the real situation. Therefore, molecular dynamics (MD) simulation was applied to take the flexibility of GSiAc molecule into account for binding energy calculation. Only five analytes with different enantioselectivity including **2Br**, **2CF3**, **2Me** (complete separation), **2F** (incomplete separation) and **2Cl** (no separation) were selected for MD simulations due to limitation in computational resources.

MD simulations were performed using the HyperChem software. MM+ force fields, set up time to simulation at 100 picoseconds, and periodic box size of 50x50x50 $Å^3$ were used in this simulation. All solvent (water) molecules was deleted. The kinetic energy (E_k), potential energy (E_p) and total energy (E) obtained from the MD simulations are given in Table 4.3.

Table 4.3 Kinetic energy (E_k), potential energy (E_p) and total energy (E) from MD simulation during 20-100 ps

compound		α	E_k	ΔE_k	E_p	ΔE_p	E	ΔE
2CF3	R	1.126	526.165	0.026	577.809	1.599	1103.974	1.573
	S		526.139		579.408		1105.547	
2Br	R	1.104	522.534	0.045	586.293	13.599	1108.827	13.554
	S		522.579		572.694		1095.273	
2Me	R	1.071	522.559	0.005	576.790	5.248	1099.349	5.253
	S		522.554		571.542		1094.096	
2F	R	1.012	522.533	0.013	580.147	3.267	1102.680	3.254
	S		522.546		576.880		1099.426	
2Cl	R	1	526.168	0.036	582.197	7.829	1108.366	7.794
	S		526.133		590.027		1116.156	

From Table 4.3, it is clearly seen that E_k values of the two enantiomers for each analyte are similar, i.e. ΔE_k is close to zero. So, ΔE_p was used to describe the separation of enantiomers instead. The **2CF3** was completely separated but it had lower ΔE_p value than those of analytes that were not separated or incompletely separated. Therefore, it

seems that results from the MD simulations could not be used for the prediction of analytes in this study. However, it is still statistically not conclusive because only five compounds were used, and thus more compounds are needed for further investigation in future works.

4.2.3 QSPR study

Initially, attempts were made to find the relationship between the alcohol descriptors and the difference of elution temperatures. When the correlation matrix was created to find the correlation, no relationship could be found. When the genetic function approximation (GFA) method was used, QSPR model with R^2 of 0.354 (Figure 4.11a) was found, however, the model is statistically not qualified.

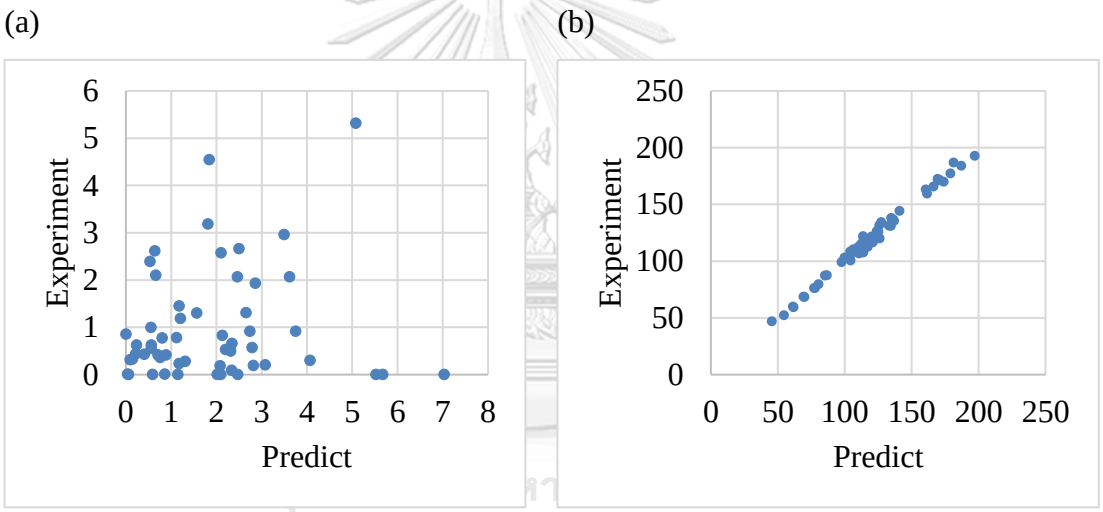

Figure 4.11 (a) The graphs show the relationship between the difference of elution temperatures obtained from the experiment and the prediction and (b) the relationship between the elution temperature of more retained enantiomer of each compound and the prediction.

As the relationship for overall compounds could not be established, the compounds were divided into 2 groups, more retained and less retained enantiomers. Then, QSPR was separately analyzed for each group. Selection of whether the descriptors of *R* or *S* are more retained or less retained were based on the docking results. The best QSPR models were created using GFA method and are shown as follow.

QSPR model for more retained enantiomers

Elution temperature = 23.50 X1 + 536.11 X2 + 4.01 X3 + 2.05 X4 - 7.36 X5 - 0.58 X6 + 140.51

R^2 = 0.991, q^2 (cross validated R^2) = 0.988

Where X1 : Binding energy (DMol3 Molecular)

X2 : HOMO energy (DMol3 Molecular)

X3 : Molecular refractivity (Fast Descriptors)

X4 : Subgraph counts (2): path (Fast Descriptors)

X5 : Methyl (Fragment Counts)

X6 : Quadrupole xz (VAMP Electrostatics)

QSPR model for less retained enantiomers

Elution temperature = 21.97 X1 + 5.15 X2 + 6.53 X3 - 21.02 X4 - 10.29 X5 - 0.64 X6 + 0.097 X7 - 2.98

R^2 = 0.993, q^2 (cross validated R^2) = 0.989

Where X1 : Hydrogen bond acceptor (Fast Descriptors)

X2 : Molecular refractivity (Fast Descriptors)

X3 : Kappa-2 (Fast Descriptors)

X4 : Kappa-1 (alpha modified) (Fast Descriptors)

X5 : E-state keys (sums): S_sssCH (Fast Descriptors)

X6 : E-state keys (sums): S_sF (Fast Descriptors)

X7 : Octupole yyy (VAMP Electrostatics)

Table 4.4 Actual and predicted values of elution temperature for both more retained and less retained enantiomers

More retained enantiomers			Less retained enantiomers		
Actual	Predicted	Residual	Actual	Predicted	Residual
100.58	104.28	-3.70	100.16	105.17	-5.01
162.97	160.61	2.36	162.06	156.86	5.20
159.48	161.49	-2.01	159.48	155.96	3.52
131.22	133.00	-1.79	131.22	130.98	0.24

More retained enantiomers			Less retained enantiomers		
Actual	Predicted	Residual	Actual	Predicted	Residual
138.03	134.59	3.45	138.03	128.91	9.12
112.43	109.96	2.48	109.25	111.77	-2.52
118.00	113.86	4.14	113.46	112.02	1.44
119.18	117.61	1.57	117.87	114.95	2.92
120.59	120.38	0.21	118.49	119.71	-1.22
103.06	99.67	3.39	101.88	100.88	1.00
169.81	173.94	-4.13	169.24	171.14	-1.90
120.03	126.04	-6.01	119.82	122.95	-3.13
99.00	97.52	1.48	99.00	97.58	1.42
121.56	120.11	1.46	118.90	117.61	1.29
118.94	120.79	-1.85	118.44	118.47	-0.03
130.85	134.53	-3.68	130.23	134.29	-4.06
46.86	45.54	1.32	46.77	43.20	3.57
107.40	113.98	-6.57	102.09	108.89	-6.80
126.43	124.00	2.43	126.12	124.10	2.02
103.75	103.96	-0.21	103.75	103.10	0.65
68.36	69.78	-1.42	68.17	67.69	0.48
59.41	61.69	-2.28	58.88	59.48	-0.60
114.51	111.92	2.59	111.90	111.28	0.62
172.36	169.43	2.93	171.59	170.24	1.35
87.44	86.71	0.73	87.44	84.23	3.21
79.52	80.40	-0.88	79.29	79.22	0.07
52.17	54.49	-2.32	51.98	51.66	0.32
110.43	106.56	3.87	110.43	107.71	2.72
116.44	118.23	-1.79	115.89	118.80	-2.91
136.84	136.08	0.75	136.18	138.43	-2.25
112.50	117.23	-4.73	112.50	110.19	2.31
131.40	125.83	5.57	130.57	127.96	2.61

More retained enantiomers			Less retained enantiomers		
Actual	Predicted	Residual	Actual	Predicted	Residual
108.27	104.15	4.13	107.42	104.14	3.28
68.53	69.13	-0.60	68.53	69.72	-1.19
59.89	61.19	-1.30	59.56	61.04	-1.48
106.82	110.77	-3.96	105.37	111.95	-6.58
171.52	170.91	0.62	171.52	170.87	0.65
87.27	85.10	2.16	87.27	87.21	0.06
76.10	77.01	-0.91	75.82	78.32	-2.50
144.34	141.03	3.31	142.27	138.56	3.71
192.70	197.24	-4.54	192.34	196.48	-4.14
135.55	136.83	-1.28	134.56	136.28	-1.72
114.60	116.07	-1.47	112.53	112.45	0.08
134.41	127.36	7.05	132.02	127.89	4.13
183.98	187.09	-3.11	183.55	186.87	-3.32
116.65	121.03	-4.38	115.35	119.46	-4.11
108.05	108.15	-0.10	105.47	106.04	-0.57
165.51	166.21	-0.70	165.08	165.80	-0.72
109.69	114.25	-4.57	107.76	111.39	-3.63
171.04	169.98	1.06	170.26	168.86	1.40
76.21	77.82	-1.61	75.79	78.53	-2.74
186.78	181.22	5.55	186.48	185.29	1.19
177.24	178.99	-1.75	176.32	176.24	0.08
125.76	125.09	0.66	125.13	124.53	0.60
121.99	113.62	8.36	119.03	117.12	1.91

The QSPR models have R^2 of 0.991 and 0.993 (Figure 4.11b) and q^2 (cross validated R^2) of 0.988 and 0.989 for more retained and less retained groups, respectively. These statistical values are very satisfactory. The highest residual value is 9.12 degrees Celsius and the average error is 2.68 and 2.30 degrees Celsius for more retained and less retained enantiomers that are very small deviation. However, since the individual enantiomer pairs have an average difference of elution temperature of just

only 1.23 degrees Celsius, which is less than the average error of this models. So, the models can be only used to predict elution temperature, not the separation of the enantiomers.

CHAPTER V
Conclusion

Enantiomeric separations of fifty-five chiral alcohols (13 aliphatic alcohols and 42 alcohols of aromatic structure) were studied by gas chromatography using a mixture of octakis(2,3-di-*O*-acetyl-6-*O*-*tert*-butyldimethylsilyl)-γ-CD (or GSiAc) in polysiloxane OV-1701 as a stationary phase. The analytes were performed under temperature program and isothermal condition. For the separations under temperature program, 44 alcohols could be separated into their enantiomers; among these, 30 alcohols could be completely separated into their enantiomers under the temperature program with resolutions of 1.5 or higher. Most of them are alcohols with one aromatic ring with substitution(s) on the aromatic ring. Among 13 aliphatic alcohols used in this study, 2-hexanol (**2hex**) was the only aliphatic alcohol that could be completely separated into their enantiomers.

Twenty-five alcohols, 1-phenylethanol analogs with substitution on the aromatic ring or substitution at the stereogenic center, were selected for further study under isothermal conditions at 6-8 different temperatures. The effect of column temperature on retention factor and enantioselectivity was investigated. The difference in enthalpy change ($\Delta\Delta H$) and the difference in entropy change ($\Delta\Delta S$) for the enantiomeric separation could be calculated. The effects of type and position of substitution on the analyte structure were also considered. For halogen-substituted 1-phenylethanols, the effect of temperature on enantioselectivity were in the order of *para* > *meta* > *ortho*. In contrast, temperature affected enantioselectivities of methyl- or trifluoromethyl-substituted alcohols at *ortho*-position more than other positions. For *para*-substituted alcohols, enantioselectivities could be improved with the decrease in column temperature with the substituent in the order of halogen > trifluoromethyl > alkyl > phenyl, respectively. The influence of column temperature on enantioselectivity of 1-phenylethanols with different type of substituent at the stereogenic center was also studied. It was found that decreasing column temperature could improve enantioselectivities of alcohols with small alkyl substitution at the stereogenic center rather than bulky alkyl or large phenyl group. Among 25 chiral alcohols in this study, enantiomers of 2-methyl-1-phenyl-1-propanol (**9**) could be baseline separated with the shortest analysis time.

For molecular docking calculations, information from binding energy between alcohols and GSiAc with substituent inside the cavity geometry optimized with PM7 method was used to find the model to qualitatively predict the separation of enantiomers. The best predictive model used $-\Delta(\Delta H_{mean})$ value, the difference of average binding energy of all 100 docked configurations between (*R*) and (*S*)

complexes. This model gave the prediction accuracy of 83.64 %, 100%, and 18.18% for overall, separable, and non-separable analytes, respectively.

MD simulations of five analytes with different separability were conducted. The E_k values of the enantiomer pairs of all analytes are similar. The ΔE_p values have no relationship with the separability. Thus, both ΔE_k and ΔE_p could not be used to predict the separation of enantiomers.

For QSPR studied, attempts to find relationship between alcohol descriptors and the difference of elution temperature for a group of all compounds were not success. Therefore, QSPR models were created separately for the more retained and the less retained enantiomers. Statistical values of the best QSPR models are very satisfactory. However, the predicted elution temperatures have the average error of 2.68 and 2.30 degrees Celsius for more retained and less retained enantiomers, respectively, which exceeds the difference in elution temperature of the enantiomer pairs. Therefore, the models can be used to predict the elution temperature but not the separation of the enantiomers.

REFERENCES

[1] Dixon, A.S.J., et al. Synthetic D(-)penicillamine in rheumatoid arthritis. Annals of the Rheumatic Diseases 34 (1975): 416-421.

[2] Hutt, A.J. and Tan, S.C. Drug chirality and its clinical significance. Drug 52(Suppl. 5) (1996): 1-12.

[3] Barrett, A.M. and Cullum, V.A. The biological properties of the optical isomers of propranolol and their effects on cardiac arrhythmias. British Journal of Pharmacology 34 (1968): 43-55.

[4] Péter, M., Péter, A., Eycken, J.V., Csomós, P., Bernáth, G., and Fülöp, F. High-performance liquid chromatographic separation of enantiomers of cyclic 1,3-amino alcohol derivatives. Journal of Chromatography A 816 (1998): 123-129.

[5] Ellington, J.J., Evans, J.J., Prickett, K.B., and Champion Jr, W.L. High-performance liquid chromatographic separation of the enantiomers of organophosphorus pesticides on polysaccharide chiral stationary phases. Journal of Chromatography A 928 (2001): 145-154.

[6] Xiu-Juan, L., Liang, Z., Yong-Fei, M., Xian-Zhi, P., Yong-Zhang, Z., and Li-Ren, C. Direct chiral separation of four indole derivatives by high performance liquid chromatography with chiral stationary phase. Chinese Journal of Analytical Chemistry 35(4) (2007): 515-519.

[7] Bjørnsdottir, I., HonoréHansen, S., and Terabe, S. Chiral separation in non-aqueous media by capillary electrophoresis using the ion-pair principle. Journal of Chromatography A 745 (1996): 37-44.

[8] Zhou, J., Ai, F., Zhou, B., Tang, J., Ng, S.C., and Tang, W. Hydroxyethylammonium monosubstituted cyclodextrin as chiral selector for capillary electrophoresis. Anal Chim Acta 800 (2013): 95-102.

[9] Marini, R.D., et al. Nonaqueous capillary electrophoresis method for the enantiomeric purity determination of *S*-timolol using heptakis(2,3-di-*O*-methyl-6-*O*-sulfo)-beta-cyclodextrin: validation using the accuracy profile strategy and estimation of uncertainty. Journal of Chromatography A 1120 (2006): 102-111.

[10] Aranyi, A., Péter, A., Ilisz, I., Fülöp, F., and Scriba, G.K.E. Cyclodextrin-mediated enantioseparation of phenylalanine amide derivatives and amino alcohols by capillary electrophoresis - Role of complexation constants and complex mobilities. Electrophoresis 35 (2014): 2848-2854.

[11] Bicchi, C., D'Amato, A., Manzin, V., Galli, A., and Galli, M. Cyclodextrin derivatives in the gas chromatographic separation of racemic mixtures of volatile compounds X. 2,3-di-*O*-ethyl-6-*O*-*tert*.-butyldimethylsilyl-beta- and -gamma-cyclodextrins. Journal of Chromatography A 742 (1996): 161-173.

[12] Takahisa, E. and Engel, K.H. 2,3-di-*O*-methoxymethyl-6-*O*-*tert*-butyldimethylsilyl-gamma-cyclodextrin: a new class of cyclodextrin derivatives for gas chromatographic separation of enantiomers. Journal of Chromatography A 1063 (2005): 181-192.

[13] Luxová, A., Urbanová, K., Valterová, I., Terzo, M., and Borg-Karlson, A.K. Absolute configuration of chiral terpenes in marking pheromones of bumblebees and cuckoo bumblebees. Chirality 16 (2004): 228-233.

[14] Liberto, E., et al. Enantiomer identification in the flavour and fragrance fields by "interactive" combination of linear retention indices from enantioselective gas chromatography and mass spectrometry. Journal of Chromatography A 1195 (2008): 117-126.

[15] Ramos, M.C.K.V., Teixeira, L.H.P., Neto, F.R.A., Barreiro, E.J., Rodrigues, C.R., and Fraga, C.A.M. Chiral separation of gamma-butyrolactone derivatives by gas chromatography on 2,3-di-*O*-methyl-6-*O*-*tert*.-butyldimethylsilyl-beta-cyclodextrin. Journal of Chromatography A 985 (2003): 321-331.

[16] Jongjitwattana, M. Enantiomeric separation of alcohols by gas chromatography using beta-cyclodextrin derivative as stationary phase. Master's Thesis, Department of Chemistry, Faculty of Science, Chulalongkorn University, 2014.

[17] Bartschat, D. and Mosandl, A. Stereoisomeric flavour compounds LXXIV 2-phenylpropanol, 2-phenylpropanal and 2-phenylpropanal dimethyl acetah structure elucidation and structure-function relationship. European Food Research and Technology 202 (1996): 226-269.

[18] Garkani-Nejad, Z. and Ahmadvand, M. Investigation of linear and nonlinear chemometrics methods in modeling of retention time of phenol derivatives based on molecular descriptors. Separation Science and Technology 46(6) (2011): 1034-1044.

[19] Fragkaki, A.G., et al. Comparison of multiple linear regression, partial least squares and artificial neural networks for prediction of gas chromatographic relative retention times of trimethylsilylated anabolic androgenic steroids. J Chromatogr A 1256 (2012): 232-9.

[20] Dashtbozorgi, Z., Golmohammadi, H., and Konoz, E. Support vector regression based QSPR for the prediction of retention time of pesticide residues in gas chromatography–mass spectroscopy. Microchemical Journal 106 (2013): 51-60.

[21] Aires-de-Sousa, J. and Gasteiger, J. Prediction of enantiomeric selectivity in chromatography Application of conformation-dependent and conformation-independent descriptors of molecular chirality. Journal of Molecular Graphics and Modelling 20 (2002): 373-388.

[22] Braiuca, P., Lorena, K., Ferrario, V., Ebert, C., and Gardossi, L. A three-dimensional quanititative structure-activity relationship (3D-QSAR) model for predicting the enantioselectivity of *Candida antarctica* Lipase B. Advanced Synthesis & Catalysis 351(9) (2009): 1293-1302.

[23] Roy, K., Kar, S., and Das, R.N. A primer on QSAR/QSPR modeling: fundamental concepts.: Cham: Springer, 2015.

[24] Juvancz, Z. The role of cyclodextrins in chiral selective chromatography. Trends in Analytical Chemistry 21 (2002): 379-388.

[25] Valle, E.M.M.D. Cyclodextrins and their uses: a review. Process Biochemistry 39 (2004): 1033-1046.

[26] Kurkov, S.V. and Loftsson, T. Cyclodextrins. Int J Pharm 453(1) (2013): 167-80.
[27] Schurig, V. and Nowotny, H.-P. Gas chromatographic separation of enantiomers on cyclodextrin derivatives. Angewandte Chemie International Edition in English 29(9) (1990): 939-957.
[28] Szejtli, J. Introduction and general overview of cyclodextrin chemistry. Chemical Reviews 98(5) (1998): 1743-1754.
[29] Maas, B., Dietrich, A., and Mosandl, A. Comparison of different 6-*tert*-butyldimethyl-silylated cyclodextrins as chiral stationary phases in GC. Journal of Microcolumn Separations 8(1) (1996): 47-56.
[30] Shitangkoon, A. and Vigh, G. Systematic modification of the separation selectivity of cyclodextrin-based gas chromatographic stationary phases by varying the size of the 6-O-substituents. Journal of Chromatography A 738(1) (1996): 31-42.
[31] Schurig, V. Separation of enantiomers by gas chromatography. Journal of Chromatography A 21 (2001): 647-661.
[32] Schurig, V. Chiral separations using gas chromatography. Trends in Analytical Chemistry 21 (2002): 647-661.
[33] Schurig, V. Enantiomer separation by gas chromatography on chiral stationary phases. Journal of Chromatography A 666 (1994): 111-129.
[34] Huang, K., Zhang, X., and Armstrong, D.W. Ionic cyclodextrins in ionic liquid matrices as chiral stationary phases for gas chromatography. Journal of Chromatography A 1217 (2010): 5261-5273.
[35] Špánik, I., Krupčik, J., and Schurig, V. Comparison of two methods for the gas chromatographic determination of thermodynamic parameters of enantioselectivity. Journal of Chromatography A 843(1-2) (1999): 123-128.
[36] Morris, G.M., et al. AutoDock 4.2 User Guide [Online]. Available from: http://autodock.scripps.edu/faqs-help/manual/autodock-4-2-user-guide [2017, June 4]
[37] Goodsell, D.S., Morris, G.M., and Olson, A.J. Automated docking of flexible ligands: Applications of AutoDock. Journal of Molecular Recognition 9 (1996): 1-5.
[38] Rapaport, D.C. The art of molecular dynamics simulation. New York: Cambridge University Press, 1997.
[39] Newton, I. Philosophiae naturalis principia mathematica. Royal Society London, 1687.
[40] Rogers, D. and Hopfinger, A.J. Application of genetic function approximation (GFA) to quantitative structure-activity relationships (QSAR) and quantitative structure-property relationships (QSPR). Journal of Chemical Information and Computer Science 34 (1994): 854-866.
[41] Rogers, D. Genetic function approximation: a genetic approach to building quantitative structure-activity models. in Proceedings of the 10th European Symposium on Quantitative Structure-Activity Relationships: QSAR and Molecular Modeling. Barcelona, Spain: Prous Scientific Publishers, 1994.
[42] Rogers, D. Development of the genetic function approximation algorithm. in Proceedings of the 6th International Conference on Genetic Algorithms. San Mateo, CA: Morgan-Kaufmann, 1995.

[43] Rogers, D. G/SPLINES: a hybrid of friedman's multivariate adaptive regression splines (MARS) algorithm with holland's genetic algorithm. in Proceedings of the Fourth International Conference on Genetic Algorithms. San Diego: Morgan-Kaufmann, 1991.

[44] Rogers, D. Data analysis using G/SPLINES. in Advances In Neural Processing Systems 4. San Mateo, CA: Morgan Kaufmann, 1992.

[45] Wold, S., Wold, H., Ruhe, A., and Dunn, W.J.I. The collinearity problem in linear regression. the partial least squares (PLS) approach to generalized inverses. SIAM Journal of Science, Statistics, and Computation 5 (1984): 735-743.

[46] Glen, W.G., Dunn, W.J.I., and Scott, D.R. Principal components analysis and partial least squares regression. Tetrahedron Computer Methodology 2 (1989): 279-356.

[47] Rumelhart, D.E., E., H.G., and J., W.R. Learning internal representations by error propagation. in Parallel Distributed Processing: Exploration into the microstructure of cognition: MA: MIT Press, Cambridge, 1986.

[48] Iamsam-ang, W. Enantiomeric seperation of aromatic alcohols by gas chromatography using derivatized beta-cyclodextrins as stationary phases. M.Sc, Department of Chemistry, Faculty of Science, Chulalongkorn University, 2002.

[49] Konghuirob, O. Enantiomeric separation of alcohols by gas chromatography using derivatized cyclodextrins as stationary phases. Master’s Thesis, Department of Chemistry, Faculty of Science, Chulalongkorn University, 2004.

[50] Stewart, J. MOPAC [Online]. 2016. Available from: http://openmopac.net/ [2017, April 9]

[51] Morris, G.M., et al. AutoDock (version 4.0.1) 2007, The Scripps Research Institute: La Jolla, CA.

[52] Sanner, M.F., et al. AutoDockTools (version 1.4.5) 2007, The Scripps Research Institute: La Jolla, CA.

APPENDIX

Table A1 Slope and y-intercept from ln k′ versus 1/T plots of 25 alcohols on the GSiAc column

analyte	temperature range (°C)	less retained enantiomer			more retained enantiomer		
		ln k′= m(1/T)+C		R^2	ln k′= m(1/T)+C		R^2
		m	C		m	C	
1	70-130	7334.13	-17.30	0.9993	7400.77	-17.46	0.9994
2F	70-130	7947.03	-18.78	0.9987	7928.72	-18.72	0.9986
3F	80-140	7472.03	-17.27	0.9993	7597.63	-17.56	0.9993
4F	80-150	7167.07	-16.55	0.9994	7516.80	-17.35	0.9991
2Cl	100-160	7788.61	-17.27	0.9987	7859.62	-17.44	0.9983
3Cl	100-160	7714.04	-16.82	0.9994	7845.77	-17.11	0.9993
4Cl	100-160	7819.68	-17.00	0.9995	8227.78	-17.91	0.9992
2Br	100-160	7976.59	-17.30	0.9987	8036.85	-17.42	0.9988
3Br	110-170	7831.84	-16.61	0.9994	7947.91	-16.87	0.9994
4Br	110-170	8012.58	-16.94	0.9995	8372.60	-17.73	0.9992
2Me	80-140	7572.29	-17.26	0.9991	8018.11	-18.30	0.9987
3Me	80-140	7016.48	-16.14	0.9991	7289.28	-16.80	0.9988
4Me	80-150	7202.78	-16.51	0.9987	7466.42	-17.11	0.9985
2CF3	80-140	7033.88	-16.62	0.9990	7841.11	-18.51	0.9982
3CF3	80-140	7628.85	-17.61	0.9994	7649.76	-17.66	0.9993
4CF3	80-150	7731.11	-17.66	0.9994	8076.35	-18.46	0.9991
4Et	90-150	7212.34	-16.11	0.9993	7395.02	-16.53	0.9992
4Bu	110-170	7602.36	-16.10	0.9995	7750.79	-16.43	0.9994
4tBu	100-160	7172.35	-15.47	0.9996	7280.31	-15.73	0.9996
4Phe	150-210	8609.51	-16.45	0.9995	8778.06	-16.80	0.9995
7	80-140	7578.55	-17.44	0.9990	8125.99	-18.72	0.9985
8	90-150	7788.66	-17.47	0.9987	8172.60	-18.35	0.9982
9	80-140	7710.29	-17.53	0.9990	8642.34	-19.73	0.9982
10	90-150	7568.25	-16.92	0.9990	7806.82	-17.47	0.9987
11	130-200	8320.14	-16.31	0.9994	8444.47	-16.57	0.9994

Table A2 Thermodynamic parameters of 25 alcohols on the GSiAc column

analyte	enthalpic term (kcal/mol)			entropic term (cal/mol×K)		
	$-\Delta H_1$	$-\Delta H_2$	$-\Delta\Delta H$	$-\Delta S_1$	$-\Delta S_2$	$-\Delta\Delta S$
1	14.57	14.71	0.13	28.86	29.18	0.32
2F	15.79	15.75	-0.04	31.80	31.69	-0.12
3F	14.85	15.10	0.25	28.79	29.37	0.58
4F	14.24	14.94	0.69	27.37	28.96	1.60
2Cl	15.48	15.62	0.14	28.81	29.14	0.34
3Cl	15.33	15.59	0.26	27.89	28.48	0.58
4Cl	15.54	16.35	0.81	28.26	30.07	1.81
2Br	15.85	15.97	0.12	28.85	29.09	0.23
3Br	15.56	15.79	0.23	27.48	28.00	0.52
4Br	15.92	16.64	0.72	28.14	29.71	1.57
2Me	15.05	15.93	0.89	28.78	30.85	2.06
3Me	13.94	14.48	0.54	26.55	27.87	1.32
4Me	14.31	14.84	0.52	27.29	28.48	1.19
2CF3	13.98	15.58	1.60	27.51	31.26	3.75
3CF3	15.16	15.20	0.04	29.47	29.58	0.11
4CF3	15.36	16.05	0.69	29.56	31.15	1.59
4Et	14.33	14.69	0.36	26.50	27.32	0.82
4Bu	15.11	15.40	0.29	26.48	27.13	0.65
4tBu	14.25	14.47	0.21	25.23	25.73	0.50
4Phe	17.11	17.44	0.33	27.18	27.87	0.69
7	15.06	16.15	1.09	29.13	31.68	2.54
8	15.48	16.24	0.76	29.19	30.95	1.76
9	15.32	17.17	1.85	29.32	33.69	4.37
10	15.04	15.51	0.47	28.10	29.20	1.11
11	16.53	16.78	0.25	26.88	27.41	0.53

Table A3 The highest operation column temperature and chromatographic parameters for 25 alcohols where enantiomers are baseline separated (Rs ≥ 1.5) on the GSiAc column.

analyte	temperature (°C)	t_{R1}	t_{R2}	k'_2	α	Rs
1	88	10.933	11.199	20.09	1.026	1.59
2F	NS	NS	NS	NS	NS	NS
3F	115	4.273	4.390	7.35	1.031	1.55
4F	144	1.536	1.580	2.00	1.043	1.52
2Cl	105	15.511	15.836	28.77	1.022	1.50
3Cl	131	5.493	5.640	9.70	1.030	1.54
4Cl	164	1.855	1.906	2.63	1.038	1.54
2Br	140	4.334	4.446	7.45	1.029	1.50
3Br	130	9.143	9.378	16.83	1.027	1.50
4Br	169	2.266	2.327	3.45	1.035	1.55
2Me	149	1.652	1.699	2.24	1.042	1.56
3Me	116	3.938	4.046	6.65	1.031	1.56
4Me	141	1.797	1.847	2.55	1.040	1.56
2CF3	153	1.037	1.069	1.05	1.063	1.56
3CF3	NS	NS	NS	NS	NS	NS
4CF3	142	1.928	1.982	2.78	1.038	1.57
4Et	136	2.874	2.948	4.66	1.031	1.50
4Bu	140	5.581	5.728	10.00	1.029	1.55
4tBu	114	11.486	11.778	21.48	1.027	1.58
4Phe	175	8.511	8.730	15.85	1.027	1.53
7	149	1.481	1.525	1.92	1.046	1.59
8	146	2.169	2.229	3.26	1.036	1.60
9	158	1.380	1.419	1.72	1.045	1.54
10	129	3.933	4.041	6.73	1.032	1.59
11	153	13.221	13.540	24.94	1.025	1.53

*NS = No enantioseparation or baseline separation could not be observed.

Example of input and output docking files

Grid parameter file (.gpf)

```
npts 60 60 60                          # num.grid points in xyz
parameter_file AD4_parameters.dat      # force field default parameter file
gridfld Host.maps.fld                  # grid_data_file
spacing 0.375                          # spacing(A)
receptor_types C OA Si                 # receptor atom types
ligand_types A C Cl F OA Br HD         # ligand atom types
receptor Host.pdbqt                    # macromolecule
gridcenter -3.928 5.768 2.502          # xyz-coordinates or auto
smooth 0.5                             # store minimum energy w/in rad(A)
map Host.A.map                         # atom-specific affinity map
map Host.C.map                         # atom-specific affinity map
map Host.Cl.map                        # atom-specific affinity map
map Host.F.map                         # atom-specific affinity map
map Host.OA.map                        # atom-specific affinity map
map Host.Br.map                        # atom-specific affinity map
map Host.HD.map                        # atom-specific affinity map
elecmap Host.e.map                     # electrostatic potential map
dsolvmap Host.d.map                    # desolvation potential map
dielectric -0.1465                     # <0, AD4 distance-dep.diel;>0, constant
```


Docking parameter file (.dpf)

```
autodock_parameter_version 4.2     # used by autodock to validate parameter set
parameter_file AD4.1_bound.dat     # parameter library filename
intelec                            # calculate internal electrostatics
seed pid time                      # seeds for random generator
ligand_types A C HD OA             # atoms types in ligand
fld Host.maps.fld                  # grid_data_file
map Host.A.map                     # atom-specific affinity map
map Host.C.map                     # atom-specific affinity map
map Host.HD.map                    # atom-specific affinity map
map Host.OA.map                    # atom-specific affinity map
elecmap Host.e.map                 # electrostatics map
```

```
desolvmap Host.d.map                # desolvation map
move Guest.pdbqt                    # small molecule
about 2.0937 1.4273 -0.0902         # small molecule center
tran0 random                        # initial coordinates/A or random
quaternion0 random                  # initial orientation
dihe0 random                        # initial dihedrals (relative) or random
torsdof 2                           # torsional degrees of freedom
rmstol 2.0                          # cluster_tolerance/A
extnrg 1000.0                       # external grid energy
e0max 0.0 10000                     # max initial energy; max number of retries
ga_pop_size 150                     # number of individuals in population
ga_num_evals 2500000                # maximum number of energy evaluations
ga_num_generations 27000            # maximum number of generations
ga_elitism 1                        # number of top individuals to survive to next
  generation
ga_mutation_rate 0.02               # rate of gene mutation
ga_crossover_rate 0.8               # rate of crossover
ga_window_size 10                   #
ga_cauchy_alpha 0.0                 # Alpha parameter of Cauchy distribution
ga_cauchy_beta 1.0                  # Beta parameter Cauchy distribution
set_ga                              # set the above parameters for GA or LGA
sw_max_its 300                      # iterations of Solis & Wets local search
sw_max_succ 4                       # consecutive successes before changing rho
sw_max_fail 4                       # consecutive failures before changing rho
sw_rho 1.0                          # size of local search space to sample
sw_lb_rho 0.01                      # lower bound on rho
ls_search_freq 0.06                 # probability of performing local search on
  individual
set_psw1                            # set the above pseudo-Solis & Wets parameters
unbound_model bound                 # state of unbound ligand
ga_run 100                          # do this many hybrid GA-LS runs
analysis                            # perform a ranked cluster analysis
```

Docking log file (.dlg)

```
AutoDock 4.2 Release 4.2.6
```

```
 (C) 1989-2012 The Scripps Research Institute
AutoDock comes with ABSOLUTELY NO WARRANTY.
AutoDock is free software, and you are welcome
to redistribute it under certain conditions;
for details type 'autodock4 -C'

          main.cc  $Revision: 1.213 $

         Compiled on Jul 18 2014 at 15:34:58


This file was created at:                4:31 23" p.m., 06/08/2016
          on host:            "GREENTEA-LENOVO"
Current Working Directory = "D:\Docking\1R"

_____________________________________________________________________

         SETTING UP DEFAULT PARAMETER LIBRARY
_____________________________________________________________________


Random number generator was seeded with values 2656, 1465378283.
Docking parameter file (DPF) used for this docking:        1R.dpf
DPF> autodock_parameter_version 4.2        # used by autodock to validate parameter
set

       Autodock parameter version 4.2.
DPF> parameter_file AD4.1_bound.dat        # parameter library filename

Using read_parameter_library() to try to open and read "AD4.1_bound.dat".

DPF> intelec                               # calculate internal electrostatics
Electrostatic energies will be calculated for all non-bonds between moving atoms.
DPF> seed pid time                         # seeds for random generator
```

```
Random number generator was seeded with values 2656, 1465378283.
DPF> ligand_types A C HD OA                # atoms types in ligand

DPF> fld CD.maps.fld                       # grid_data_file

Opening Grid Map Dimensions file:          CD.maps.fld
Grid Point Spacing =                       0.375 Angstroms

Even Number of User-specified Grid Points =        60 x-points
                                                   60 y-points
                                                   60 z-points

Coordinates of Central Grid Point of Maps =(-3.928, 5.768, 2.502)
Macromolecule file used to create Grid Maps =      CD.pdbqt
Grid Parameter file used to create Grid Maps =     CHOFClBr.gpf
Minimum coordinates in grid = (-15.178, -5.482, -8.748)
Maximum coordinates in grid = (7.322, 17.018, 13.752)

DPF> map CD.A.map                  # atom-specific affinity map

DPF> map CD.C.map                  # atom-specific affinity map

DPF> map CD.HD.map                 # atom-specific affinity map

DPF> map CD.OA.map                 # atom-specific affinity map

DPF> elecmap CD.e.map              # electrostatics map

DPF> desolvmap CD.d.map            # desolvation map

DPF> move 1R.pdbqt                 # small molecule

1,4-interactions will be _ignored_ in the non-bonded internal energy calculation.

Ligand PDBQT file = "1R.pdbqt"
```

INPUT LIGAND PDBQT FILE:

INPUT-LIGAND-PDBQT: REMARK 2 active torsions:

INPUT-LIGAND-PDBQT: REMARK status: ('A' for Active; 'I' for Inactive)

INPUT-LIGAND-PDBQT: REMARK 1 A between atoms: C_3 and C_7

INPUT-LIGAND-PDBQT: REMARK 2 A between atoms: C_7 and O_9

INPUT-LIGAND-PDBQT: ROOT

INPUT-LIGAND-PDBQT: ATOM 1 C UNK A 1 0.000 0.000 0.000 0.00 0.00 0.004 A

INPUT-LIGAND-PDBQT: ATOM 2 C UNK A 1 1.383 0.000 0.000 0.00 0.00 -0.029 A

INPUT-LIGAND-PDBQT: ATOM 3 C UNK A 1 2.086 1.195 0.000 0.00 0.00 -0.033 A

INPUT-LIGAND-PDBQT: ATOM 4 C UNK A 1 1.392 2.392 0.016 0.00 0.00 0.039 A

INPUT-LIGAND-PDBQT: ATOM 5 C UNK A 1 -0.692 1.199 0.005 0.00 0.00 -0.005 A

INPUT-LIGAND-PDBQT: ATOM 6 C UNK A 1 0.008 2.392 0.016 0.00 0.00 0.002 A

INPUT-LIGAND-PDBQT: ENDROOT

INPUT-LIGAND-PDBQT: BRANCH 3 7

INPUT-LIGAND-PDBQT: ATOM 7 C UNK A 1 3.600 1.182 -0.049 0.00 0.00 0.285 C

INPUT-LIGAND-PDBQT: ATOM 8 C UNK A 1 4.089 0.852 -1.469 0.00 0.00 -0.020 C

INPUT-LIGAND-PDBQT: BRANCH 7 9

INPUT-LIGAND-PDBQT: ATOM 9 O UNK A 1 4.056 2.496 0.335 0.00 0.00 -0.556 OA

INPUT-LIGAND-PDBQT: ATOM 10 H UNK A 1 5.015 2.565 0.244 0.00 0.00 0.314 HD

INPUT-LIGAND-PDBQT: ENDBRANCH 7 9

INPUT-LIGAND-PDBQT: ENDBRANCH 3 7

INPUT-LIGAND-PDBQT: TORSDOF 2

```
Total charge on ligand                    =   +0.001 e
REMARK  2 active torsions:
REMARK  status: ('A' for Active; 'I' for Inactive)
REMARK    1  A    between atoms: C_3  and  C_7
REMARK    2  A    between atoms: C_7  and  O_9


Number of Rotatable Bonds in Small Molecule =     2 torsions
Number of atoms in ligand:  10

Number of non-hydrogen atoms in ligand:  9

Number of vibrational degrees of freedom of ligand:  24


Number of torsional degrees of freedom = 2
Estimated loss of torsional free energy upon binding = +0.5488 kcal/mol


DPF> about 2.0937 1.4273 -0.0902          # small molecule center

Small molecule center of rotation =   (+2.094, +1.427, -0.090)

DPF> tran0 random                         # initial coordinates/A or random

Initial translation =                     (-14.081, 13.758, 8.335) Angstroms
DPF> quaternion0 random                   # initial orientation

Each run will begin with a new, random initial orientation.
Initial quaternion,  (x,y,z,w) =          ( -0.290, 0.748, -0.149, -0.578 ),
DPF> dihe0 random                         # initial dihedrals (relative) or random

DPF> torsdof 2                            # torsional degrees of freedom

Number of torsional degrees of freedom = 2
```

Free energy coefficient for torsional degrees of freedom = 0.2744 as specified in parameter library "AD4.1_bound.dat".

Estimated loss of torsional free energy upon binding = +0.5488 kcal/mol

DPF> rmstol 2.0 # cluster_tolerance/A

Maximum RMS tolerance for conformational cluster analysis = 2.00 Angstroms

DPF> extnrg 1000.0 # external grid energy

External grid energy (beyond grid map walls) = 1000.00

DPF> e0max 0.0 10000 # max initial energy; max number of retries

Using user-specified maximum number of retries for simanneal initialization, 10000 retries.

If the simanneal initial energy is greater than e0max, 0.000,

then a new, random initial state will be created.

DPF> ga_pop_size 150 # number of individuals in population

A population of 150 individuals will be used

DPF> ga_num_evals 2500000 # maximum number of energy evaluations

There will be at most 2500000 function evaluations used.

DPF> ga_num_generations 27000 # maximum number of generations

The GA will run for at most 27000 generations.

DPF> ga_elitism 1 # number of top individuals to survive to next generation

The 1 best will be preserved each GA generation.

DPF> ga_mutation_rate 0.02 # rate of gene mutation

The mutation rate is 0.020000.
DPF> ga_crossover_rate 0.8 # rate of crossover

The crossover rate is 0.800000.
DPF> ga_window_size 10 #

The GA's selection window is 10 generations.
DPF> ga_cauchy_alpha 0.0 # Alpha parameter of Cauchy distribution

The alpha parameter (for the Cauchy distribution) is being set to 0.000000.
DPF> ga_cauchy_beta 1.0 # Beta parameter Cauchy distribution

The beta parameter (for the Cauchy distribution) is being set to 1.000000.
DPF> set_ga # set the above parameters for GA or LGA

DPF> sw_max_its 300 # iterations of Solis & Wets local search

Solis & Wets algorithms will perform at most 300 iterations.
DPF> sw_max_succ 4 # consecutive successes before changing rho

Solis & Wets algorithms expand rho every 4 in a row successes.
DPF> sw_max_fail 4 # consecutive failures before changing rho

Solis & Wets algorithms contract rho every 4 in a row failures.
DPF> sw_rho 1.0 # size of local search space to sample

rho is set to 1.000000.
DPF> sw_lb_rho 0.01 # lower bound on rho

rho will never get smaller than 0.010000.
DPF> ls_search_freq 0.06 # probability of performing local search on individual

Local search will be performed with frequency 0.060000.
DPF> set_psw1 # set the above pseudo-Solis & Wets parameters

Creating a new Local Search object using the pseudo-Solis-Wets algorithm (pSW1) with the current settings.

DPF> unbound_model bound # state of unbound ligand

DPF> ga_run 100 # do this many hybrid GA-LS runs

centering ligand on specified point: 2.094 1.427 -0.090
Furthest true ligand atom from "about" center is 3.153 Angstroms (maxrad).
Number of requested GA dockings = 100 runs
Unbound model to be used is 'same as bound' [AutoDock 4.2 default].

BEGINNING GENETIC ALGORITHM DOCKING 1 of 100
Run: 1 Seed: 1654790642 335888396 [Run 1 of 100 GA/GALS]
Beginning LAMARCKIAN GENETIC ALGORITHM (LGA), with a maximum of 2500000 energy evaluations.

Final-Value: -3.099

FINAL GENETIC ALGORITHM DOCKED STATE
_____

Detailed state: trans -2.482 -1.228 -3.259 quatxyzw -0.836053 0.172125 -0.344676 -0.390624 center 2.094 1.427 -0.090 ntor 2 -144.1436 77.6379
State: -2.482 -1.228 -3.259 -0.908 0.187 -0.374 -134.013 -144.14 77.64

DOCKED: MODEL 1
DOCKED: USER Run = 1
DOCKED: USER DPF = 1R.dpf
DOCKED: USER
DOCKED: USER Estimated Free Energy of Binding = -2.48 kcal/mol [=(1)+(2)+(3)-(4)]

```
DOCKED: USER    Estimated Inhibition Constant, Ki  = 15.22 mM (millimolar)
[Temperature = 298.15 K]
DOCKED: USER
DOCKED: USER    (1) Final Intermolecular Energy     =   -3.03 kcal/mol
DOCKED: USER        vdW + Hbond + desolv Energy =   -2.93 kcal/mol
DOCKED: USER        Electrostatic Energy                =   -0.09 kcal/mol
DOCKED: USER    (2) Final Total Internal Energy     =   -0.07 kcal/mol
DOCKED: USER    (3) Torsional Free Energy           =   +0.55 kcal/mol
DOCKED: USER    (4) Unbound System's Energy  [=(2)] =   -0.07 kcal/mol
DOCKED: USER
DOCKED: USER
DOCKED: USER    NEWDPF move 1R.pdbqt
DOCKED: USER    NEWDPF about 2.093700 1.427300 -0.090200
DOCKED: USER    NEWDPF tran0 -2.482024 -1.228239 -3.259123
DOCKED: USER    NEWDPF quaternion0 -0.836053 0.172125 -0.344676 -0.390624
DOCKED: USER    NEWDPF axisangle0 -0.908210 0.186980 -0.374424 -
134.013323
DOCKED: USER    NEWDPF quat0 -0.908210 0.186980 -0.374424 -134.013323
DOCKED: USER    NEWDPF dihe0 -144.14 77.64
DOCKED: USER  keepresnum = 1
DOCKED: USER
DOCKED: REMARK  2 active torsions:
DOCKED: REMARK  status: ('A' for Active; 'I' for Inactive)
DOCKED: REMARK   1  A    between atoms: C_3  and  C_7
DOCKED: REMARK    2  A    between atoms: C_7  and  O_9
DOCKED: USER                                    x      y       z     vdW  Elec   q    Type
DOCKED: USER                                   ____   ____   ____  ____  ____  ___  ___
DOCKED: ROOT
DOCKED: ATOM      1  C   UNK A   1      -3.864   0.894  -3.124 -0.39 -0.00    +0.004
A
DOCKED: ATOM      2  C   UNK A   1      -2.891   0.123  -2.513 -0.39 +0.01    -0.029
A
DOCKED: ATOM      3  C   UNK A   1      -2.419  -1.028  -3.124 -0.41 +0.01    -
0.033 A
DOCKED: ATOM      4  C   UNK A   1      -2.918  -1.394  -4.362 -0.22 -0.00
+0.039 A
```

DOCKED: ATOM 5 C UNK A 1 -4.369 0.520 -4.357 -0.28 +0.00 -0.005 A

DOCKED: ATOM 6 C UNK A 1 -3.891 -0.623 -4.974 -0.21 -0.00 +0.002 A

DOCKED: ENDROOT

DOCKED: BRANCH 3 7

DOCKED: ATOM 7 C UNK A 1 -1.389 -1.889 -2.423 -0.27 -0.03 +0.285 C

DOCKED: ATOM 8 C UNK A 1 -1.493 -3.348 -2.900 -0.23 +0.00 -0.020 C

DOCKED: BRANCH 7 9

DOCKED: ATOM 9 O UNK A 1 -0.088 -1.358 -2.748 -0.21 +0.12 -0.556 OA

DOCKED: ATOM 10 H UNK A 1 -0.099 -0.392 -2.732 -0.34 -0.18 +0.314 HD

DOCKED: ENDBRANCH 7 9

DOCKED: ENDBRANCH 3 7

DOCKED: TORSDOF 2

DOCKED: TER

DOCKED: ENDMDL

BEGINNING GENETIC ALGORITHM DOCKING 2 of 100

Run: 2 Seed: 104725381 1836320293 [Run 2 of 100 GA/GALS]

Beginning LAMARCKIAN GENETIC ALGORITHM (LGA), with a maximum of 2500000 energy evaluations.

Final-Value: -3.096

.

.

.

BEGINNING GENETIC ALGORITHM DOCKING 100 of 100

Run: 100 Seed: 2002407305 1823102030 [Run 100 of 100 GA/GALS]

Beginning LAMARCKIAN GENETIC ALGORITHM (LGA), with a maximum of 2500000 energy evaluations.

Final-Value: -3.105

FINAL GENETIC ALGORITHM DOCKED STATE

DPF> analysis # perform a ranked cluster analysis

CLUSTER ANALYSIS OF CONFORMATIONS

Number of conformations = 100

RMSD cluster analysis will be performed using the ligand atoms only (10 / 10 total atoms).

Outputting structurally similar clusters, ranked in order of increasing energy.

Number of distinct conformational clusters found = 11, out of 100 runs,
Using an rmsd-tolerance of 2.0 A

CLUSTERING HISTOGRAM

Clus	Lowest	Run	Mean	Num	Histogram

```
-ter    | Binding |       | Binding   | in    |
Rank | Energy   |       | Energy    | Clus |   5     10      15     20      25      30      35
_____|_________|____|_________|_____|____:____|____:____|____:____|____:_____
_
  1    |    -2.56    | 69  |    -2.48   | 72
|#######################################
  2    |    -2.45    | 54 |    -2.43   |  2  |##
  3    |    -2.36    | 28 |    -2.28   |  9 |#########
  4    |    -2.32    | 50 |    -2.27   |  5 |#####
  5    |    -2.32    |  9 |    -2.30   |  2 |##
  6    |    -2.30    | 93 |    -2.30   |  1 |#
  7    |    -2.29    | 63 |    -2.25   |  3 |###
  8    |    -2.27    | 40 |    -2.21   |  3 |###
  9    |    -2.24    | 77 |    -2.24   |  1 |#
 10    |    -2.17    | 34 |    -2.17   |  1 |#
 11    |    -2.15    | 20 |    -2.15   |  1 |#
_____|_________|___|_________|___|_____________________________________________
```

Number of multi-member conformational clusters found = 7, out of 100 runs.

RMSD TABLE

_____

Rank	Sub-Rank	Run	Binding Energy	Cluster RMSD	Reference RMSD	Grep Pattern
1	1	69	-2.56	0.00	5.60	RANKING
1	2	32	-2.56	0.05	5.61	RANKING
1	3	78	-2.56	0.15	5.55	RANKING
1	4	97	-2.55	0.15	5.61	RANKING
1	5	72	-2.54	0.13	5.61	RANKING
1	6	46	-2.54	0.07	5.64	RANKING

1	7	58	-2.54	0.12	5.59	RANKING
1	8	47	-2.54	0.18	5.61	RANKING
1	9	53	-2.53	0.13	5.65	RANKING
1	10	84	-2.53	0.22	5.66	RANKING
1	11	91	-2.53	0.25	5.64	RANKING
1	12	90	-2.51	0.15	5.68	RANKING
1	13	88	-2.51	1.49	5.73	RANKING
1	14	74	-2.51	0.29	5.59	RANKING
1	15	75	-2.50	1.51	5.77	RANKING
1	16	41	-2.50	1.50	5.70	RANKING
1	17	65	-2.50	1.49	5.69	RANKING
1	18	71	-2.50	0.17	5.65	RANKING
1	19	31	-2.50	0.49	5.73	RANKING
1	20	15	-2.50	0.34	5.73	RANKING
1	21	12	-2.50	1.48	5.70	RANKING
1	22	22	-2.50	1.48	5.67	RANKING
1	23	33	-2.49	1.49	5.71	RANKING
1	24	100	-2.49	1.48	5.69	RANKING
1	25	79	-2.49	1.49	5.71	RANKING
1	26	39	-2.49	1.51	5.78	RANKING
1	27	81	-2.49	1.50	5.75	RANKING
1	28	49	-2.49	1.52	5.75	RANKING
1	29	36	-2.49	1.52	5.76	RANKING
1	30	76	-2.49	1.48	5.65	RANKING
1	31	57	-2.49	1.50	5.84	RANKING
1	32	60	-2.48	0.22	5.69	RANKING
1	33	2	-2.48	1.51	5.89	RANKING
1	34	44	-2.48	1.46	5.74	RANKING
1	35	51	-2.48	1.50	5.70	RANKING
1	36	62	-2.48	1.51	5.73	RANKING
1	37	13	-2.48	1.51	5.70	RANKING
1	38	10	-2.48	1.47	5.65	RANKING
1	39	56	-2.48	0.20	5.68	RANKING
1	40	59	-2.48	1.55	5.92	RANKING
1	41	1	-2.48	1.49	5.70	RANKING

1	42	37	-2.48	1.46	5.73	RANKING
1	43	43	-2.48	1.48	5.69	RANKING
1	44	99	-2.48	1.48	5.68	RANKING
1	45	6	-2.48	1.52	5.89	RANKING
1	46	45	-2.48	0.22	5.66	RANKING
1	47	8	-2.48	1.51	5.87	RANKING
1	48	21	-2.47	1.47	5.74	RANKING
1	49	89	-2.47	1.52	5.89	RANKING
1	50	26	-2.47	1.47	5.71	RANKING
1	51	11	-2.47	1.51	5.88	RANKING
1	52	4	-2.47	1.49	5.68	RANKING
1	53	38	-2.47	1.49	5.70	RANKING
1	54	25	-2.47	1.49	5.69	RANKING
1	55	23	-2.47	1.52	5.89	RANKING
1	56	27	-2.47	0.23	5.64	RANKING
1	57	87	-2.47	1.48	5.72	RANKING
1	58	96	-2.46	1.50	5.72	RANKING
1	59	66	-2.46	0.29	5.71	RANKING
1	60	3	-2.46	1.50	5.82	RANKING
1	61	30	-2.46	1.49	5.71	RANKING
1	62	14	-2.46	1.47	5.73	RANKING
1	63	42	-2.46	1.49	5.72	RANKING
1	64	85	-2.46	1.46	5.74	RANKING
1	65	92	-2.46	1.49	5.72	RANKING
1	66	52	-2.45	1.47	5.79	RANKING
1	67	55	-2.45	1.47	5.65	RANKING
1	68	48	-2.43	1.49	5.82	RANKING
1	69	29	-2.43	1.50	5.74	RANKING
1	70	67	-2.40	1.51	5.85	RANKING
1	71	17	-2.32	0.53	5.86	RANKING
1	72	80	-2.32	1.56	5.89	RANKING
2	1	54	-2.45	0.00	7.77	RANKING
2	2	19	-2.40	0.22	7.74	RANKING
3	1	28	-2.36	0.00	5.72	RANKING
3	2	82	-2.32	0.10	5.70	RANKING

3	3	94	-2.31	0.30	5.73	RANKING
3	4	86	-2.27	1.94	6.42	RANKING
3	5	18	-2.26	0.80	5.63	RANKING
3	6	16	-2.25	0.44	5.79	RANKING
3	7	98	-2.25	0.41	5.81	RANKING
3	8	5	-2.23	1.29	5.93	RANKING
3	9	35	-2.22	1.23	5.96	RANKING
4	1	50	-2.32	0.00	8.36	RANKING
4	2	73	-2.30	0.75	7.96	RANKING
4	3	70	-2.29	0.38	8.37	RANKING
4	4	68	-2.28	0.54	8.34	RANKING
4	5	95	-2.16	1.76	8.27	RANKING
5	1	9	-2.32	0.00	7.08	RANKING
5	2	64	-2.28	0.21	7.15	RANKING
6	1	93	-2.30	0.00	5.15	RANKING
7	1	63	-2.29	0.00	16.37	RANKING
7	2	83	-2.28	0.19	16.34	RANKING
7	3	24	-2.19	1.23	16.25	RANKING
8	1	40	-2.27	0.00	8.63	RANKING
8	2	7	-2.27	0.04	8.61	RANKING
8	3	61	-2.11	0.92	9.04	RANKING
9	1	77	-2.24	0.00	7.38	RANKING
10	1	34	-2.17	0.00	11.81	RANKING
11	1	20	-2.15	0.00	16.32	RANKING

INFORMATION ENTROPY ANALYSIS FOR THIS CLUSTERING

Information entropy for this clustering = 0.25 (rmstol = 2.00 Angstrom)

STATISTICAL MECHANICAL ANALYSIS

Partition function, Q = 100.41 at Temperature, T = 298.15 K
Free energy, A ~ -2730.90 kcal/mol at Temperature, T = 298.15 K
Internal energy, U = -2.42 kcal/mol at Temperature, T = 298.15 K
Entropy, S = 9.15 kcal/mol/K at Temperature, T = 298.15 K

LOWEST ENERGY DOCKED CONFORMATION from EACH CLUSTER

Keeping original residue number (specified in the input PDBQ file) for outputting.

MODEL 69
USER Run = 69
USER Cluster Rank = 1
USER Number of conformations in this cluster = 72
USER
USER RMSD from reference structure = 5.600 A
USER
USER Estimated Free Energy of Binding = -2.56 kcal/mol [=(1)+(2)+(3)-(4)]
USER Estimated Inhibition Constant, Ki = 13.26 mM (millimolar) [Temperature = 298.15 K]
USER
USER (1) Final Intermolecular Energy = -3.11 kcal/mol
USER vdW + Hbond + desolv Energy = -2.89 kcal/mol
USER Electrostatic Energy = -0.22 kcal/mol
USER (2) Final Total Internal Energy = -0.07 kcal/mol
USER (3) Torsional Free Energy = +0.55 kcal/mol
USER (4) Unbound System's Energy [=(2)] = -0.07 kcal/mol

```
USER
USER
USER
USER    DPF = 1R.dpf
USER    NEWDPF move       1R.pdbqt
USER    NEWDPF about      2.093700 1.427300 -0.090200
USER    NEWDPF tran0      -1.885959 -1.547956 -2.889779
USER    NEWDPF axisangle0         0.713043 -0.623856 -0.319959 -70.917470
USER    NEWDPF quaternion0        0.413648 -0.361909 -0.185613 -0.814534
USER    NEWDPF dihe0      20.48 15.66
USER
USER                        x      y      z   vdW   Elec       q     RMS
ATOM     1  C   UNK A   1      -3.358  -1.177  -4.921 -0.20 -0.00    +0.004     5.600
ATOM     2  C   UNK A   1      -2.433  -2.009  -4.318 -0.19 +0.00    -0.029     5.600
ATOM     3  C   UNK A   1      -1.959  -1.729  -3.045 -0.35 +0.00    -0.033     5.600
ATOM     4  C   UNK A   1      -2.432  -0.615  -2.374 -0.29 -0.01    +0.039     5.600
ATOM     5  C   UNK A   1      -3.821  -0.057  -4.251 -0.31 +0.00    -0.005     5.600
ATOM     6  C   UNK A   1      -3.358   0.218  -2.977 -0.45 -0.00    +0.002     5.600
ATOM     7  C   UNK A   1      -0.909  -2.621  -2.415 -0.24 -0.03    +0.285     5.600
ATOM     8  C   UNK A   1       0.501  -2.095  -2.728 -0.38 +0.00    -0.020     5.600
ATOM     9  O   UNK A   1      -1.133  -2.611  -0.989 -0.13 +0.05    -0.556     5.600
ATOM    10  H   UNK A   1      -0.316  -2.807  -0.514 -0.35 -0.23    +0.314     5.600
TER
ENDMDL
MODEL      54
USER    Run = 54
USER    Cluster Rank = 2
USER    Number of conformations in this cluster = 2
USER
USER    RMSD from reference structure       = 7.775 A
USER
USER    Estimated Free Energy of Binding    =   -2.45 kcal/mol  [=(1)+(2)+(3)-(4)]
USER    Estimated Inhibition Constant, Ki   =   15.90 mM (millimolar)  [Temperature
= 298.15 K]
USER
```

```
USER    (1) Final Intermolecular Energy     =   -3.00 kcal/mol
USER        vdW + Hbond + desolv Energy     =   -2.83 kcal/mol
USER        Electrostatic Energy            =   -0.18 kcal/mol
USER    (2) Final Total Internal Energy     =   -0.04 kcal/mol
USER    (3) Torsional Free Energy           =   +0.55 kcal/mol
USER    (4) Unbound System's Energy  [=(2)] =   -0.04 kcal/mol
USER
USER
USER
USER    DPF = 1R.dpf
USER    NEWDPF move       1R.pdbqt
USER    NEWDPF about      2.093700 1.427300 -0.090200
USER    NEWDPF tran0      -1.383381 5.610279 6.347332
USER    NEWDPF axisangle0         0.517930 -0.714176 0.470852 -56.457327
USER    NEWDPF quaternion0        0.244976 -0.337799 0.222709 -0.881067
USER    NEWDPF dihe0      165.01 -56.19
USER
USER                        x       y       z   vdW   Elec       q     RMS
ATOM      1  C   UNK A   1     -2.039   3.968   4.530 -0.35 -0.00    +0.004     7.775
ATOM      2  C   UNK A   1     -1.109   4.282   5.504 -0.23 +0.01    -0.029     7.775
ATOM      3  C   UNK A   1     -1.303   5.375   6.335 -0.34 +0.01    -0.033     7.775
ATOM      4  C   UNK A   1     -2.445   6.142   6.194 -0.29 -0.02    +0.039     7.775
ATOM      5  C   UNK A   1     -3.176   4.744   4.383 -0.50 +0.00    -0.005     7.775
ATOM      6  C   UNK A   1     -3.376   5.828   5.219 -0.47 -0.00    +0.002     7.775
ATOM      7  C   UNK A   1     -0.253   5.737   7.366 -0.11 -0.04    +0.285     7.775
ATOM      8  C   UNK A   1      1.100   5.104   7.001 -0.20 +0.00    -0.020     7.775
ATOM      9  O   UNK A   1     -0.137   7.175   7.377 -0.02 +0.14    -0.556     7.775
ATOM     10  H   UNK A   1     -0.622   7.563   6.638 -0.31 -0.27    +0.314     7.775
TER
ENDMDL
MODEL       28
USER    Run = 28
USER    Cluster Rank = 3
USER    Number of conformations in this cluster = 9
USER
```

```
USER    RMSD from reference structure       = 5.716 A
USER
USER    Estimated Free Energy of Binding    =   -2.36 kcal/mol  [=(1)+(2)+(3)-(4)]
USER    Estimated Inhibition Constant, Ki   =   18.66 mM (millimolar)  [Temperature
= 298.15 K]
USER
USER    (1) Final Intermolecular Energy     =   -2.91 kcal/mol
USER        vdW + Hbond + desolv Energy     =   -2.76 kcal/mol
USER        Electrostatic Energy            =   -0.14 kcal/mol
USER    (2) Final Total Internal Energy     =   -0.06 kcal/mol
USER    (3) Torsional Free Energy           =   +0.55 kcal/mol
USER    (4) Unbound System's Energy  [=(2)] =   -0.06 kcal/mol
USER
USER
USER
USER    DPF = 1R.dpf
USER    NEWDPF move       1R.pdbqt
USER    NEWDPF about      2.093700 1.427300 -0.090200
USER    NEWDPF tran0      5.497076 5.623935 -3.439804
USER    NEWDPF axisangle0         0.506815 0.698286 -0.505504 89.529697
USER    NEWDPF quaternion0        0.356899 0.491732 -0.355975 0.710003
USER    NEWDPF dihe0      129.81 171.53
USER
USER                      x      y      z    vdW   Elec       q    RMS
ATOM     1  C   UNK A   1      5.081   3.143  -3.123 -0.33 +0.00    +0.004     5.716
ATOM     2  C   UNK A   1      5.445   4.327  -2.509 -0.30 +0.00    -0.029     5.716
ATOM     3  C   UNK A   1      5.445   5.517  -3.221 -0.31 +0.00    -0.033     5.716
ATOM     4  C   UNK A   1      5.062   5.514  -4.550 -0.21 -0.00    +0.039     5.716
ATOM     5  C   UNK A   1      4.709   3.141  -4.457 -0.31 -0.00    -0.005     5.716
ATOM     6  C   UNK A   1      4.698   4.329  -5.165 -0.24 +0.00    +0.002     5.716
ATOM     7  C   UNK A   1      5.892   6.800  -2.550 -0.21 -0.02    +0.285     5.716
ATOM     8  C   UNK A   1      4.706   7.766  -2.393 -0.37 +0.00    -0.020     5.716
ATOM     9  O   UNK A   1      6.415   6.449  -1.252 -0.12 +0.16    -0.556     5.716
ATOM    10  H   UNK A   1      5.831   5.822  -0.806 -0.35 -0.29    +0.314     5.716
TER
```

```
ENDMDL
MODEL      50
USER    Run = 50
USER    Cluster Rank = 4
USER    Number of conformations in this cluster = 5
USER
USER    RMSD from reference structure       = 8.361 A
USER
USER    Estimated Free Energy of Binding    =   -2.32 kcal/mol  [=(1)+(2)+(3)-(4)]
USER    Estimated Inhibition Constant, Ki   =   19.94 mM (millimolar)  [Temperature
= 298.15 K]
USER
USER    (1) Final Intermolecular Energy     =   -2.87 kcal/mol
USER        vdW + Hbond + desolv Energy     =   -2.73 kcal/mol
USER        Electrostatic Energy            =   -0.14 kcal/mol
USER    (2) Final Total Internal Energy     =   -0.07 kcal/mol
USER    (3) Torsional Free Energy           =   +0.55 kcal/mol
USER    (4) Unbound System's Energy  [=(2)] =   -0.07 kcal/mol
USER
USER
USER
USER    DPF = 1R.dpf
USER    NEWDPF move       1R.pdbqt
USER    NEWDPF about      2.093700 1.427300 -0.090200
USER    NEWDPF tran0      -1.626822 5.391105 6.612271
USER    NEWDPF axisangle0         0.374767 -0.819605 -0.433355 157.773431
USER    NEWDPF quaternion0        0.367740 -0.804236 -0.425229 0.192749
USER    NEWDPF dihe0      -73.18 168.34
USER
USER                         x       y       z    vdW   Elec       q     RMS
ATOM      1  C   UNK A   1      0.823   5.836   7.091 -0.18 -0.00    +0.004     8.361
ATOM      2  C   UNK A   1     -0.083   5.244   6.230 -0.26 +0.00    -0.029     8.361
ATOM      3  C   UNK A   1     -1.447   5.383   6.440 -0.33 +0.01    -0.033     8.361
ATOM      4  C   UNK A   1     -1.896   6.134   7.512 -0.23 -0.01    +0.039     8.361
ATOM      5  C   UNK A   1      0.371   6.577   8.170 -0.13 +0.00    -0.005     8.361
```

```
ATOM      6  C   UNK A   1      -0.989   6.725   8.374 -0.16 -0.00    +0.002     8.361
ATOM      7  C   UNK A   1      -2.429   4.691   5.518 -0.36 -0.13    +0.285     8.361
ATOM      8  C   UNK A   1      -3.267   5.726   4.750 -0.62 +0.01    -0.020     8.361
ATOM      9  O   UNK A   1      -1.662   3.894   4.591 -0.22 +0.18    -0.556     8.361
ATOM     10  H   UNK A   1      -1.803   2.952   4.752 -0.24 -0.21    +0.314     8.361
TER
ENDMDL
MODEL        9
USER    Run = 9
USER    Cluster Rank = 5
USER    Number of conformations in this cluster = 2
USER
USER    RMSD from reference structure       = 7.084 A
USER
USER    Estimated Free Energy of Binding    =   -2.32 kcal/mol  [=(1)+(2)+(3)-(4)]
USER    Estimated Inhibition Constant, Ki   =   20.05 mM (millimolar)  [Temperature
= 298.15 K]
USER
USER    (1) Final Intermolecular Energy     =   -2.87 kcal/mol
USER        vdW + Hbond + desolv Energy     =   -2.65 kcal/mol
USER        Electrostatic Energy            =   -0.22 kcal/mol
USER    (2) Final Total Internal Energy     =   -0.07 kcal/mol
USER    (3) Torsional Free Energy           =   +0.55 kcal/mol
USER    (4) Unbound System's Energy  [=(2)] =   -0.07 kcal/mol
USER
USER
USER
USER    DPF = 1R.dpf
USER    NEWDPF move       1R.pdbqt
USER    NEWDPF about      2.093700 1.427300 -0.090200
USER    NEWDPF tran0      -1.949865 -3.992912 3.281236
USER    NEWDPF axisangle0          0.644996 -0.601114 -0.471850 138.587178
USER    NEWDPF quaternion0         0.603332 -0.562285 -0.441371 0.353580
USER    NEWDPF dihe0      -81.21 99.73
USER
```

```
USER                    x      y      z    vdW   Elec       q     RMS
ATOM     1  C   UNK A   1     -0.502  -2.975   5.097 -0.31 -0.00    +0.004     7.084
ATOM     2  C   UNK A   1     -0.533  -3.481   3.810 -0.28 -0.00    -0.029     7.084
ATOM     3  C   UNK A   1     -1.732  -3.880   3.240 -0.31 +0.00    -0.033     7.084
ATOM     4  C   UNK A   1     -2.904  -3.751   3.963 -0.25 -0.00    +0.039     7.084
ATOM     5  C   UNK A   1     -1.675  -2.858   5.822 -0.28 +0.00    -0.005     7.084
ATOM     6  C   UNK A   1     -2.874  -3.244   5.250 -0.31 -0.00    +0.002     7.084
ATOM     7  C   UNK A   1     -1.745  -4.478   1.848 -0.20 -0.01    +0.285     7.084
ATOM     8  C   UNK A   1     -3.164  -4.940   1.476 -0.23 +0.00    -0.020     7.084
ATOM     9  O   UNK A   1     -1.306  -3.453   0.933 -0.12 +0.07    -0.556     7.084
ATOM    10  H   UNK A   1     -0.395  -3.610   0.655 -0.36 -0.27    +0.314     7.084
TER
ENDMDL
MODEL      93
USER    Run = 93
USER    Cluster Rank = 6
USER    Number of conformations in this cluster = 1
USER
USER    RMSD from reference structure       = 5.150 A
USER
USER    Estimated Free Energy of Binding    =   -2.30 kcal/mol  [=(1)+(2)+(3)-(4)]
USER    Estimated Inhibition Constant, Ki   =   20.76 mM (millimolar)  [Temperature
= 298.15 K]
USER
USER    (1) Final Intermolecular Energy     =   -2.84 kcal/mol
USER        vdW + Hbond + desolv Energy     =   -2.78 kcal/mol
USER        Electrostatic Energy            =   -0.07 kcal/mol
USER    (2) Final Total Internal Energy     =   -0.07 kcal/mol
USER    (3) Torsional Free Energy           =   +0.55 kcal/mol
USER    (4) Unbound System's Energy  [=(2)] =   -0.07 kcal/mol
USER
USER
USER
USER    DPF = 1R.dpf
USER    NEWDPF move       1R.pdbqt
```

```
USER    NEWDPF about       2.093700 1.427300 -0.090200
USER    NEWDPF tran0       4.860719 4.567411 -3.340072
USER    NEWDPF axisangle0          -0.550386 0.833588 -0.046959 -145.365782
USER    NEWDPF quaternion0         -0.525439 0.795803 -0.044830 -0.297660
USER    NEWDPF dihe0       89.28 -92.01
USER
USER                         x      y      z   vdW   Elec       q     RMS
ATOM      1  C   UNK A   1      6.630   5.763  -1.972 -0.22 -0.00    +0.004     5.150
ATOM      2  C   UNK A   1      6.256   4.569  -2.562 -0.24 +0.00    -0.029     5.150
ATOM      3  C   UNK A   1      5.098   4.493  -3.321 -0.35 -0.00    -0.033     5.150
ATOM      4  C   UNK A   1      4.325   5.627  -3.498 -0.29 +0.00    +0.039     5.150
ATOM      5  C   UNK A   1      5.849   6.893  -2.142 -0.30 +0.00    -0.005     5.150
ATOM      6  C   UNK A   1      4.699   6.821  -2.908 -0.35 -0.00    +0.002     5.150
ATOM      7  C   UNK A   1      4.673   3.169  -3.922 -0.28 +0.01    +0.285     5.150
ATOM      8  C   UNK A   1      5.844   2.172  -3.908 -0.22 -0.00    -0.020     5.150
ATOM      9  O   UNK A   1      3.585   2.661  -3.123 -0.22 -0.04    -0.556     5.150
ATOM     10  H   UNK A   1      3.920   2.166  -2.364 -0.32 -0.04    +0.314     5.150
TER
ENDMDL
MODEL      63
USER    Run = 63
USER    Cluster Rank = 7
USER    Number of conformations in this cluster = 3
USER
USER    RMSD from reference structure       = 16.366 A
USER
USER    Estimated Free Energy of Binding    =   -2.29 kcal/mol  [=(1)+(2)+(3)-(4)]
USER    Estimated Inhibition Constant, Ki   =   21.08 mM (millimolar)  [Temperature
= 298.15 K]
USER
USER    (1) Final Intermolecular Energy     =   -2.84 kcal/mol
USER        vdW + Hbond + desolv Energy     =   -2.63 kcal/mol
USER        Electrostatic Energy            =   -0.20 kcal/mol
USER    (2) Final Total Internal Energy     =   -0.07 kcal/mol
USER    (3) Torsional Free Energy           =   +0.55 kcal/mol
```

```
USER    (4) Unbound System's Energy  [=(2)] =   -0.07 kcal/mol
USER
USER
USER
USER    DPF = 1R.dpf
USER    NEWDPF move       1R.pdbqt
USER    NEWDPF about      2.093700 1.427300 -0.090200
USER    NEWDPF tran0      -7.484709 14.663605 4.272475
USER    NEWDPF axisangle0         0.975915 0.069088 -0.206920 -135.117292
USER    NEWDPF quaternion0        0.902010 0.063856 -0.191250 -0.381738
USER    NEWDPF dihe0      -52.72 -116.51
USER
USER                         x      y      z   vdW   Elec      q    RMS
ATOM      1  C   UNK A   1     -9.808  15.663   4.092 -0.15 -0.00    +0.004    16.366
ATOM      2  C   UNK A   1     -8.537  15.621   3.547 -0.15 +0.00    -0.029    16.366
ATOM      3  C   UNK A   1     -7.579  14.762   4.064 -0.29 +0.00    -0.033    16.366
ATOM      4  C   UNK A   1     -7.909  13.934   5.122 -0.33 -0.00    +0.039    16.366
ATOM      5  C   UNK A   1    -10.132  14.841   5.157 -0.22 +0.00    -0.005    16.366
ATOM      6  C   UNK A   1     -9.180  13.976   5.667 -0.32 -0.00    +0.002    16.366
ATOM      7  C   UNK A   1     -6.177  14.760   3.490 -0.29 -0.06    +0.285    16.366
ATOM      8  C   UNK A   1     -6.223  14.882   1.958 -0.43 +0.00    -0.020    16.366
ATOM      9  O   UNK A   1     -5.478  15.890   4.053 -0.10 +0.20    -0.556    16.366
ATOM     10  H   UNK A   1     -4.608  15.626   4.378 -0.35 -0.34    +0.314    16.366
TER
ENDMDL
MODEL       40
USER    Run = 40
USER    Cluster Rank = 8
USER    Number of conformations in this cluster = 3
USER
USER    RMSD from reference structure       = 8.632 A
USER
USER    Estimated Free Energy of Binding    =   -2.27 kcal/mol  [=(1)+(2)+(3)-(4)]
USER    Estimated Inhibition Constant, Ki   =   21.79 mM (millimolar)  [Temperature
= 298.15 K]
```

```
USER
USER    (1) Final Intermolecular Energy     =   -2.82 kcal/mol
USER        vdW + Hbond + desolv Energy     =   -2.79 kcal/mol
USER        Electrostatic Energy            =   -0.03 kcal/mol
USER    (2) Final Total Internal Energy     =   -0.07 kcal/mol
USER    (3) Torsional Free Energy           =   +0.55 kcal/mol
USER    (4) Unbound System's Energy  [=(2)] =   -0.07 kcal/mol
USER
USER
USER
USER    DPF = 1R.dpf
USER    NEWDPF move       1R.pdbqt
USER    NEWDPF about      2.093700 1.427300 -0.090200
USER    NEWDPF tran0      -4.551664 6.573911 -3.419045
USER    NEWDPF axisangle0         0.906283 -0.415266 -0.078775 166.245265
USER    NEWDPF quaternion0        0.899762 -0.412278 -0.078208 0.119745
USER    NEWDPF dihe0      -90.47 115.50
USER
USER                        x      y      z   vdW   Elec      q     RMS
ATOM      1  C   UNK A   1      -4.826   9.014  -2.789 -0.40 +0.00    +0.004     8.632
ATOM      2  C   UNK A   1      -3.930   8.014  -3.120 -0.23 -0.00    -0.029     8.632
ATOM      3  C   UNK A   1      -4.384   6.751  -3.469 -0.28 -0.00    -0.033     8.632
ATOM      4  C   UNK A   1      -5.744   6.502  -3.499 -0.23 +0.00    +0.039     8.632
ATOM      5  C   UNK A   1      -6.187   8.759  -2.809 -0.30 -0.00    -0.005     8.632
ATOM      6  C   UNK A   1      -6.641   7.503  -3.167 -0.26 +0.00    +0.002     8.632
ATOM      7  C   UNK A   1      -3.391   5.651  -3.782 -0.30 +0.03    +0.285     8.632
ATOM      8  C   UNK A   1      -4.107   4.443  -4.408 -0.29 -0.00    -0.020     8.632
ATOM      9  O   UNK A   1      -2.429   6.189  -4.714 -0.19 -0.00    -0.556     8.632
ATOM     10  H   UNK A   1      -1.652   6.522  -4.248 -0.30 -0.05    +0.314     8.632
TER
ENDMDL
MODEL       77
USER    Run = 77
USER    Cluster Rank = 9
USER    Number of conformations in this cluster = 1
```

```
USER
USER    RMSD from reference structure       = 7.383 A
USER
USER    Estimated Free Energy of Binding    =   -2.24 kcal/mol  [=(1)+(2)+(3)-(4)]
USER    Estimated Inhibition Constant, Ki   =   22.94 mM (millimolar)  [Temperature
= 298.15 K]
USER
USER    (1) Final Intermolecular Energy     =   -2.79 kcal/mol
USER        vdW + Hbond + desolv Energy     =   -2.55 kcal/mol
USER        Electrostatic Energy            =   -0.23 kcal/mol
USER    (2) Final Total Internal Energy     =   -0.07 kcal/mol
USER    (3) Torsional Free Energy           =   +0.55 kcal/mol
USER    (4) Unbound System's Energy  [=(2)] =   -0.07 kcal/mol
USER
USER
USER
USER    DPF = 1R.dpf
USER    NEWDPF move        1R.pdbqt
USER    NEWDPF about       2.093700 1.427300 -0.090200
USER    NEWDPF tran0       -0.938531 -3.524965 4.766614
USER    NEWDPF axisangle0          -0.755285 -0.588877 -0.287695 -96.466520
USER    NEWDPF quaternion0         -0.563339 -0.439222 -0.214581 -0.666100
USER    NEWDPF dihe0       74.70 133.91
USER
USER                        x       y       z    vdW   Elec       q     RMS
ATOM      1  C   UNK A   1      -3.177  -4.268   3.836 -0.22 -0.00    +0.004     7.383
ATOM      2  C   UNK A   1      -2.455  -3.979   4.979 -0.24 +0.00    -0.029     7.383
ATOM      3  C   UNK A   1      -1.155  -3.505   4.889 -0.28 +0.00    -0.033     7.383
ATOM      4  C   UNK A   1      -0.588  -3.308   3.642 -0.28 +0.00    +0.039     7.383
ATOM      5  C   UNK A   1      -2.604  -4.080   2.589 -0.28 +0.00    -0.005     7.383
ATOM      6  C   UNK A   1      -1.311  -3.598   2.498 -0.35 -0.00    +0.002     7.383
ATOM      7  C   UNK A   1      -0.358  -3.238   6.149 -0.15 -0.03    +0.285     7.383
ATOM      8  C   UNK A   1       0.655  -2.106   5.915 -0.31 +0.00    -0.020     7.383
ATOM      9  O   UNK A   1      -1.293  -2.856   7.179 -0.07 +0.18    -0.556     7.383
ATOM     10  H   UNK A   1      -1.305  -1.897   7.291 -0.36 -0.38    +0.314     7.383
```

```
TER
ENDMDL
MODEL      34
USER    Run = 34
USER    Cluster Rank = 10
USER    Number of conformations in this cluster = 1
USER
USER    RMSD from reference structure       = 11.808 A
USER
USER    Estimated Free Energy of Binding    =   -2.17 kcal/mol  [=(1)+(2)+(3)-(4)]
USER    Estimated Inhibition Constant, Ki   =   25.49 mM (millimolar)  [Temperature
= 298.15 K]
USER
USER    (1) Final Intermolecular Energy     =   -2.72 kcal/mol
USER        vdW + Hbond + desolv Energy     =   -2.62 kcal/mol
USER        Electrostatic Energy            =   -0.10 kcal/mol
USER    (2) Final Total Internal Energy     =   -0.08 kcal/mol
USER    (3) Torsional Free Energy           =   +0.55 kcal/mol
USER    (4) Unbound System's Energy  [=(2)] =   -0.08 kcal/mol
USER
USER
USER
USER    DPF = 1R.dpf
USER    NEWDPF move       1R.pdbqt
USER    NEWDPF about      2.093700 1.427300 -0.090200
USER    NEWDPF tran0      -9.127658 -1.877163 5.110397
USER    NEWDPF axisangle0         0.912811 -0.123161 0.389368 165.340977
USER    NEWDPF quaternion0        0.905352 -0.122155 0.386186 0.127575
USER    NEWDPF dihe0      62.83 167.59
USER
USER                        x       y       z    vdW   Elec       q     RMS
ATOM      1  C   UNK A   1     -10.293   0.143   4.116 -0.41 -0.00    +0.004    11.808
ATOM      2  C   UNK A   1      -9.364  -0.299   5.040 -0.28 -0.00    -0.029    11.808
ATOM      3  C   UNK A   1      -9.038  -1.645   5.120 -0.29 -0.00    -0.033    11.808
ATOM      4  C   UNK A   1      -9.640  -2.543   4.257 -0.18 +0.00    +0.039    11.808
```

```
ATOM      5  C   UNK A   1     -10.902  -0.759   3.260 -0.28 +0.00    -0.005    11.808
ATOM      6  C   UNK A   1     -10.570  -2.100   3.332 -0.20 +0.00    +0.002    11.808
ATOM      7  C   UNK A   1      -8.055  -2.123   6.169 -0.21 +0.01    +0.285    11.808
ATOM      8  C   UNK A   1      -6.801  -2.711   5.501 -0.34 +0.00    -0.020    11.808
ATOM      9  O   UNK A   1      -7.694  -0.982   6.975 -0.12 -0.04    -0.556    11.808
ATOM     10  H   UNK A   1      -6.769  -0.743   6.834 -0.31 -0.06    +0.314    11.808
TER
ENDMDL
MODEL       20
USER    Run = 20
USER    Cluster Rank = 11
USER    Number of conformations in this cluster = 1
USER
USER    RMSD from reference structure       = 16.316 A
USER
USER    Estimated Free Energy of Binding    =   -2.15 kcal/mol  [=(1)+(2)+(3)-(4)]
USER    Estimated Inhibition Constant, Ki   =   26.69 mM (millimolar)  [Temperature
= 298.15 K]
USER
USER    (1) Final Intermolecular Energy     =   -2.70 kcal/mol
USER        vdW + Hbond + desolv Energy     =   -2.64 kcal/mol
USER        Electrostatic Energy            =   -0.06 kcal/mol
USER    (2) Final Total Internal Energy     =   -0.07 kcal/mol
USER    (3) Torsional Free Energy           =   +0.55 kcal/mol
USER    (4) Unbound System's Energy  [=(2)] =   -0.07 kcal/mol
USER
USER
USER
USER    DPF = 1R.dpf
USER    NEWDPF move       1R.pdbqt
USER    NEWDPF about      2.093700 1.427300 -0.090200
USER    NEWDPF tran0      -6.946917 15.090980 4.572550
USER    NEWDPF axisangle0         0.128061 -0.928234 -0.349259 -137.418160
USER    NEWDPF quaternion0        0.119320 -0.864881 -0.325421 -0.363104
USER    NEWDPF dihe0      3.54 176.88
```

```
USER
USER                    x      y      z   vdW   Elec      q    RMS
ATOM    1  C   UNK A   1     -5.571  14.976   2.446 -0.39 -0.00   +0.004   16.316
ATOM    2  C   UNK A   1     -6.550  14.364   3.207 -0.42 +0.00   -0.029   16.316
ATOM    3  C   UNK A   1     -7.012  14.961   4.370 -0.31 +0.00   -0.033   16.316
ATOM    4  C   UNK A   1     -6.496  16.185   4.757 -0.18 -0.00   +0.039   16.316
ATOM    5  C   UNK A   1     -5.049  16.196   2.841 -0.27 +0.00   -0.005   16.316
ATOM    6  C   UNK A   1     -5.517  16.798   3.995 -0.18 -0.00   +0.002   16.316
ATOM    7  C   UNK A   1     -8.050  14.257   5.221 -0.25 -0.02   +0.285   16.316
ATOM    8  C   UNK A   1     -9.416  14.950   5.084 -0.25 +0.00   -0.020   16.316
ATOM    9  O   UNK A   1     -8.140  12.895   4.753 -0.08 +0.09   -0.556   16.316
ATOM   10  H   UNK A   1     -8.881  12.439   5.171 -0.31 -0.13   +0.314   16.316
TER
ENDMDL

AVSFLD: # AVS field file
AVSFLD: #
AVSFLD: # Created by AutoDock
AVSFLD: #
AVSFLD: ndim=2          # number of dimensions in the field
AVSFLD: nspace=1        # number of physical coordinates
AVSFLD: veclen=7        # vector size
AVSFLD: dim1=10         # atoms
AVSFLD: dim2=11         # conformations
AVSFLD: data=Real       # data type (byte,integer,Real,double)
AVSFLD: field=uniform   # field coordinate layout
AVSFLD: label= x y z vdW Elec q RMS
AVSFLD: variable 1 file = 1R.dlg.pdb filetype = ascii offset = 5 stride = 12
AVSFLD: variable 2 file = 1R.dlg.pdb filetype = ascii offset = 6 stride = 12
AVSFLD: variable 3 file = 1R.dlg.pdb filetype = ascii offset = 7 stride = 12
AVSFLD: variable 4 file = 1R.dlg.pdb filetype = ascii offset = 8 stride = 12
AVSFLD: variable 5 file = 1R.dlg.pdb filetype = ascii offset = 9 stride = 12
AVSFLD: variable 6 file = 1R.dlg.pdb filetype = ascii offset = 10 stride = 12
AVSFLD: variable 7 file = 1R.dlg.pdb filetype = ascii offset = 11 stride = 12
AVSFLD: # end of file
```

```
>>> Closing the docking parameter file (DPF)...
This docking finished at:                    5:09 41" p.m., 06/08/2016


_____________________________________________________________________
autodock4: Successful Completion on "GREENTEA-LENOVO"

Real= 38m 18.70s,  CPU= 1m 47.30s,  System= 1.24s
_____________________________________________________________________
```

VITA

Mister Kittiyakorn Toboonpha was born on Wednesday, September 26th, 1990 in Ratchaburi, Thailand. He graduated from Phrapathom Witthayalai School, concentration in Science and Mathematic in 2009. Then, he entered at Department of Curriculum and Instruction, Faculty of Education, Chulalongkorn University and received Bachelor of Education degree in Science after five years of study. In 2014, he continued his graduate study for a Master of Science degree in Chemistry concentration in Analytical Chemistry. His contact address is 55/581 IdeO Wutthakat Condominium, Ratchapluk Rd., Bangkho, Jomthong, Bangkok 10150.